MICROPLASTIC GENERATION IN THE MARINE ENVIRONMENT THROUGH DEGRADATION AND FRAGMENTATION

by

MIRIAM ELAINE PERRYMAN

(Under the Direction of Jenna R. Jambeck)

ABSTRACT

Plastic use has become requisite in our global economy; as population continues to increase, so too, will plastic production. At its end-of-life, some amount of plastic is mismanaged and ends up in the ocean. Once there, various environmental stresses eventually fragment plastic into microplastic pieces, now ubiquitous in the marine environment. Microplastics pose a serious threat to marine biota and possibly humans. Though the general mechanisms of microplastic formation are known, the rate and extent is not. Currently, no standard methodology for testing the formation of microplastic exists. We developed a replicable and flexible methodology for testing the formation of microplastics. We used this methodology to test the effects of UV, thermal, and mechanical stress on various types of plastic. We tested for fragmentation by measuring weight and size distribution, and looked for signs of degraded plastic using Fourier transform infrared spectroscopy. Though our results did not find any signs of fragmentation, we did see degradation. Additionally, we established a sound methodology and provided a benchmark for additional studies.

INDEX WORDS: Photo-oxidative degradation, thermal degradation, mechanical degradation, polypropylene, polyethylene, weathering-induced fragmentation, microfiber contamination, marine debris

MICROPLASTIC GENERATION IN THE MARINE ENVIRONMENTAL THROUGH DEGRADATION AND FRAGMENTATION

by

MIRIAM ELAINE PERRYMAN

B.S. Env.E., The University of Georgia, 2013

A Thesis Submitted to the Graduate Faculty of The University of Georgia in Partial Fulfillment of the Requirements for the Degree

MASTER OF SCIENCE

ATHENS, GEORGIA

2015

MICROPLASTIC GENERATION IN THE MARINE ENVIRONMENT THROUGH DEGRADATION AND FRAGMENTATION

by

MIRIAM ELAINE PERRYMAN

Major Professor: Jenna Jambeck

Committee: Jason Locklin
Bill Miller
Brock Woodson

Electronic Version Approved:

Suzanne Barber
Dean of the Graduate School
The University of Georgia
August 2015

Table of Contents

List of Figures

List of Tables

Chapter 1: Introduction

Since the mid 1940's the United States has been mass producing plastics, and today worldwide plastic production exceeds 299 million metric tons (MMT) (PlasticsEurope 2014). The widespread use of plastic can be traced to its ability to be cheaply yet durably engineered; its durability, though, can be a double edged sword as the period of time required for plastic to fully physically degrade has been reported to be anywhere from years to multiple centuries (Barnes et al. 2009). Because of this, it is arguable that every piece of plastic ever manufactured remains on earth today. This longevity can cause problems in both terrestrial and marine environments when not properly managed. Particularly, plastic accumulation in the marine environment has become of increasing concern because of its ubiquity and diffuse ecological impacts. While plastic accounts for an average of 10% of the municipal waste stream worldwide (Hoornweg and Bhada-Tata 2012), it accounts for 50-80% of marine waste (Barnes et al. 2009). Of this municipal plastic waste, it was estimated that 4.8 – 12.7 MMT entered the ocean in 2010 (Jambeck et al. 2015). Though it is uncertain how long, or even if, this plastic will completely degrade, it is known that due to certain environmental stresses the plastic will embrittle and fragment into smaller microplastic pieces (Barnes et al. 2009, Andrady 2015).

Microplastic is defined as plastic smaller than 5mm in diameter (Arther et al. 2008). There are two classes of microplastics in the ocean: those that were manufactured to be micro in size and enter the ocean directly and those that are produced from the degradation and fragmentation of macroplastic (plastics >5mm in diameter) already present in the ocean. It is this form of microplastic, termed secondary microplastic, which is likely to increase with increasing plastic production, use, and disposal. Plastic in the ocean has many deleterious effects, including absorbing and concentrating persistent organic pollutants (POPs) such as polychlorinated byphenols (PCBs), dichlorodiphenyldichloroethylenes

(DDEs), and nonylphenyls (Mato et al. 2001) , entangling and being ingested by various marine species (Derraik 2002), and providing vector transport (Gregory 2009). Microplastics in particular pose a potentially serious threat to marine species; plastic fragments ≤20µm may be ingested by a wide variety or organisms including zooplankton and krill which establish the base of the food web (Teuten et al. 2007, Andrady 2011). This provides a viable route of exposure for these sorbed POPs to enter species' tissue, bioaccumulate through the food web, and even be ingested by humans (Mato et al. 2001, Engler 2012, Rochman et al. 2014).

Many studies have identified and quantified marine microplastic. However, the disparate methodologies used to do so make comparison between studies and thus a more comprehensive understanding of the scope of the issue nearly impossible (Hidalgo-Ruz et al. 2012, Löder and Gerdts 2015). Additionally, while we know that in the marine environment, UV, thermal, and mechanical stresses all play some role in inducing degradation and fragmentation of plastic (Barnes et al. 2009, Andrady 2015), we do not know precisely the timescale or extent of this fragmentation process. Thus, our objective was to establish a replicable and widely applicable methodology for testing and quantifying microplastics. We also used this methodology to test the individual effects of each of the most predominant forms of degradation in the marine environment on plastic in a controlled setting. Specifically, three of the most ubiquitous types of polymer in the marine environment were exposed to thermal stress alone and UV and thermal stress for one year, and polypropylene was exposed to mechanical stress and abrasion for various periods of time. These polymers were tested for signs of degradation and fragmentation.

Chapter 2: Background & Literature Review

We now live in the "Plastic Age" where plastic is essential to everyday life, found in items from clothing to cars. Plastics are cheaply manufactured, durable, hygienic, and their chemical and physical properties are easily manipulated to suit a variety of needs. Plastic sealants insulate homes, a multitude of components in cars and trucks are made lighter through the use of plastic, and plastic has had a marked effect on the medical field by both reducing cost and increasing hygiene. However, the qualities of plastic that make it the material of choice in many industries also make it popular as single use, disposable packaging. The worldwide production of plastic reached 299 million metric tons (MMT) in 2013, nearly 40% of which was packaging (PlasticsEurope 2014). Several classes of plastic are commonly used in packaging: polyethylene (PE), polypropylene (PP), polystyrene (PS), and poly(ethylene terephthalate) (PET) (Andrady 2011). Low-density polyethylene (LDPE), high-density polyethylene (HDPE) and PP comprise 17%, 21%, and 24% of plastic production, respectively. LDPE is used in plastic bags, six-pack rings, bottles, and netting and HDPE in milk and juice jugs, and PP is used in rope, bottle caps, and netting (Andrady 2011).

At its end-of-life a majority of this plastic is properly managed in a landfill, materials recovery facility, or energy recovery facility. It is, however, inevitable that some amount will end up in the ocean. Of the approximately 275 MMT of plastic waste produced in 2010, 31.9 MMT was classified as mismanaged, and it is estimated that between 4.8 and 12.7 MMT of this mismanaged plastic entered the ocean. In a business as usual scenario, the cumulative amount entering the ocean is projected to increase by an order of magnitude by 2025 (Jambeck et al. 2015). Land-based sources of plastic are expected to account for a majority of marine plastic debris; however the fishing industry, which has largely switched to plastic gear (primarily PE, PP, and nylon) (Timmers et al. 2005, Watson et al. 2006)

likely contributes substantially as well (Andrady 2011). Plastic also accounts for a disproportionate share of marine debris: while plastic makes up an average of 10% of the municipal waste stream worldwide (Hoornweg and Bhada-Tata 2012), it accounts for 50-80% of marine waste (Barnes et al. 2009) and is now found in every marine environment including floating at the surface, in sea floor sediments, on beaches, and even in arctic sea ice (Barnes et al. 2009), (Obbard et al. 2014).

A myriad of ecological impacts are associated with this mass of plastic debris polluting the ocean (Kühn et al. 2015). These include absorbing and concentrating persistent organic pollutants (POPs) such as polychlorinated byphenols (PCBs), dichlorodiphenyldichloroethylenes (DDEs), and nonylphenyls (Mato et al. 2001, Rochman 2015), entangling and being ingested by various marine species (Derraik 2002), and providing a means of invasive species transport (Gregory 2009). A comprehensive analysis of the ecological consequences of plastic in the ocean, however, requires an understanding of their ultimate fate. Plastic less dense than seawater (mainly PP and PE) will float, while plastic that has either become fouled with biota or other debris or that is more dense than seawater, will sink (Andrady 2011, Ye and Andrady 1991). Global estimates of floating plastic are between 6,350 and 245,000 MMT (Cózar et al. 2014, Eriksen et al. 2014), and concentrations in the North Atlantic Gyre are equivalent to as much as 580,000 pieces per square kilometer (Law et al. 2010). While plastic on the seafloor is much harder to quantify, plastic debris has been found on ocean shelves, ridges, and even in deep basins and canyons (Pham et al. 2014).

Regardless of whether it sinks, floats, or stays suspended in between, once plastic enters the marine environment it is exposed to various stresses including UV light, heat, and mechanical abrasion that induce weathering (Barnes et al. 2009). This weathered plastic eventually degrades and fragments, forming secondary microplastics. Microplastics have been defined as being less than 5mm in diameter, recognizing 333µm as the practical lower limit when neuston nets are used for sampling (Arther et al. 2008). Because of this lower limit, studies show that a majority of the number of floating plastic particles

are not collected when using the standard neuston net sampling scheme (Syberg et al. 2015), therefore the true extent of microplastics in the ocean is not fully understood.

Two forms of microplastics exist in the ocean: primary and secondary. Primary plastics are those that were manufactured to be micro in size such as cosmetic exfoliates, sandblasting media, or even polyester fibers such as those used in fleece jackets. These microplastics are introduced to the ocean directly via runoff or pass unfiltered through the wastewater treatment system. Secondary microplastics are those that are formed through the weathering, degradation and eventual fragmentation of larger plastic debris that already exist in the ocean. Microplastics have been found everywhere looked, including in beach sediments (do Sul et al. 2009, Browne et al. 2010), ocean floor sediments (Van Cauwenberghe et al. 2013, Woodall et al. 2014), and floating on the surface (Martinez et al. 2009, Law et al. 2010). Though it is not known which form of microplastic is the dominant marine contaminant, many corporations have voluntarily agreed to phase out the use of primary microplastics in their products, and regulations mandating these eliminations have been enacted (Hitchings 2014). Though the primary microplastics that already exist in the marine environment may persist and other forms of primary microplastic will still be manufactured, these eliminations will reduce the number of primary microplastics in the marine system (Syberg et al. 2015). With no regulation of other manufactured plastics, a business as usual scenario anticipates an increase in the amount of mismanaged plastic to enter the ocean; thus, the formation of secondary microplastics may be the prevailing mechanism of oceanic influx in the future.

Similar to larger plastic debris, microplastics can absorb POPs (Mato et al. 2001), transport vectors (Löder and Gerdts 2015), and because of their smaller size are available for ingestion by biota at much lower trophic levels. Demonstrated ecological effects of marine microplastic debris include ingestion of and subsequent hepatic stress and bioaccumulation of sorbed chemicals in fish (Rochman et al. 2013), accumulation and persistence of ingested microplastic in the circulatory system of mussels

(Browne et al. 2008), and decreased weight and feeding activity along with bioaccumulation of PCBs following ingestion of microplastics by lugworms (Besseling et al. 2012). Though the risks of microplastics to the marine ecosystem are only recently recognized and poorly understood (Löder and Gerdts 2015), there is evidence that microplastics can transport POPs through the marine food web and even to humans (Engler 2012).

Before we can understand the full extent of the ecological consequences of marine microplastic we need to know the scope of the problem, including the formation of secondary microplastic. This is a complex problem. As mentioned, studies using the standard neuston net collection scheme are not detecting floating microplastics less than 333µm in diameter (Syberg et al. 2015). In addition, the vast variability in microplastic size, shape, color, and chemical and physical properties, coupled with the diverse areas of accumulation in the marine environment, makes widespread, comprehensive sampling a challenge. While studies have been conducted to identify and quantify marine microplastic debris in these areas of accumulation such as in sediments, at the sea surface, and in the water column, the myriad of disparate methodologies used make comparing the resulting datasets nearly impossible (Hidalgo-Ruz et al. 2012, Löder and Gerdts 2015). In order to better understand the fate and impact of plastic in the marine environment, it is critical to understand the mechanisms responsible for the presence of secondary microplastics. While we recognize the general mechanism, the rate and extent of microplastic formation through degradation and fragmentation remains undetermined.

Estimates of the longevity of plastic in the ocean vary from hundreds to thousands of years (Barnes et al. 2009). Though complete physical degradation is slow, polymers in the marine environment do weather and fragment (Thompson et al. 2004). Polymer degradation is defined as the chemical, physical, or biological processes resulting in bond breakage and subsequent chemical reactions. As plastics become weathered, they degrade and eventually become brittle enough to fragment into smaller and smaller pieces (Andrady 2011, Andrady 2015). For plastics in the marine environment the

predominant form of stress is UV light, a photo-oxidative degradation initiated through UV-induced photolysis of C-C and C-H bonds and propagated through a free radical mechanism of auto-oxidation (Singh and Sharma 2008). Thermal and mechanical stresses are also prominent in plastic degradation and will play a role. In most conditions, thermal and photo degradation are both classified as forms of oxidative degradation. The differences are the mechanisms of initiation that lead to the auto-oxidation cycle, and that thermal degradation occurs through either random or chain end degradation, thus is classified as a bulk phenomenon, while photo degradation generally occurs as a surface phenomenon (Singh and Sharma 2008). Mechanical degradation is generally initiated by shear or mechanical force but propagation is also supported by other chemical reactions. In the marine environment this means that excessive stress will cause the formation of two radicals (Singh and Sharma 2008); the hydrogen radical will react with oxygen to form a peroxy radical, a common intermediate in the degradation of hydrocarbons (American Meteorological Society 2012). In fact, plastic particles with linear fractures caused by mechanical stress are shown undergo higher levels of oxidation than plastics with pits or conchoidal fractures, indicating that particles that undergo mechanical erosion also undergo more extensive chemical degradation (Cooper and Corcoran 2010), (Corcoran et al. 2009). Though biodegradation in these environments may also be likely, the microbial species able to metabolize polymers are rare and this process is several orders of magnitude slower compared to light-induced oxidative degradation (Andrady 2011). Thus the rate of biodegradation is considered negligible for this study.

Plastic below the surface will likely degrade more slowly because of the lack of light and oxygen availability (Barnes et al. 2009). Additionally, a notable difference between the photo-oxidative degradation of plastics on the beach versus floating in seawater has been demonstrated (Andrady 1990, Andrady et al. 1993). Degradation in seawater is severely retarded by the lower temperatures in water compared with temperatures on land. Because sand has a relatively low specific heat (664J/kg·˚C),

beaches and therefore the plastic on them can reach temperatures well over 100˚F. The rate of photo-oxidative degradation is increased with temperature by a factor depending on the activation energy (E_a) of the process. If, for example, E_a is ~50kJ/mol, the rate of degradation doubles for every 10˚C (50˚F) increase in temperature (Andrady 2011). Thus, it is reasonable to assume that plastic lying on beaches or in the intertidal zones will undergo degradation and fragmentation at a faster rate than plastic floating in the ocean or submerged below the surface.

Though it is known that marine debris will eventually fragment, the rate and extent of this process is not well understood. As a necessary step in understanding the availability of microplastics in the marine environment, we developed a methodology to test secondary microplastic generation from various marine stresses. We determined the isolated effects of thermal only, UV and thermal together, and wave-induced mechanical stress both with and without the abrasive force of sand, on various types of plastic (HDPE, LDPE, and PP). To test for degradation and fragmentation, in particular, we looked at changes in weight, sieve size count, and size distribution determined by dynamic light scattering (DLS); both are practiced methods used in determining particle size distribution (Murdock et al. 2008, Kato et al. 2009). DLS is used to discern the sizes of Brownian nanoparticles up to a size of approximately 1-10μm (Berne and Pecora 2000). To determine particle size distribution the DLS system repeatedly illuminates the particles in a solution with a laser and analyzes the intensity fluctuations in the scattered light. Smaller particles move more quickly than larger particles, causing the intensity of the scattered light to fluctuate more quickly. This particle movement is due to Brownian motion and is defined by the Stokes-Einstein equation. The system will measure the rate and intensity of fluctuation to calculate the size of the particles based on these relationships. The system measures the size by percent relative intensity distribution; though volume and then number distribution can be generated from this using Mie theory, small errors in data gathering can lead to huge errors through this conversion (Malvern Instuments 2004). Therefore we report results in terms of intensity distribution.

In order for plastic to fragment, it must first degrade to the point of embrittlement (Andrady 2015). To test for degradation that may not have manifested in fragmentation, we tested the plastic after it had been exposed to the various stresses using attenuated total reflectance Fourier transform infrared spectroscopy (ATR-FTIR). FTIR is used to determine the molecular make up of a material. The FTIR system emits an infrared beam that passes through, is reflected, or is absorbed by the sample. Only specific frequencies of energy will be absorbed and this provides a uniquely characteristic "fingerprint" for each sample analyzed. The resulting beam next enters a detector designed to measure the special signal, and this signal is then sent to a computer where Fourier transformation takes place and the final infrared spectrum is constructed (Thermo Nicolet 2001). In ATR-FTIR the infrared beam is directed onto an optically dense crystal at a certain angle. This beam is bent and protrudes a few microns above the crystal surface and into the sample. Thus, there must be direct contact between the sample and the crystal for this technique to be successful. Again, in regions where the sample absorbs the energy the signal will be altered. This signal is passed back to the crystal and then to the detector. This method was used as it results in faster sampling and improves sample to sample reproducibility (PerkinElmer 2005).

Because UV and thermal degradation are both oxidative processes, any early signs of degradation (generally oxidation of tertiary carbons in the polyolefin chain) can be seen through absorbance in the 1640-1840cm^{-1} (carbonyl peak) band regions (Chiellini et al. 2006, Ojeda et al. 2011). Furthermore, gel permeation chromatographic (GPC) studies show that at high levels of shear stress due to mechanical stress and abrasion, PP can produce oxidation products (Li et al. 2005). Thus, FTIR can be used to test for degradation by looking specifically in the carbonyl region for signs of oxidation. This method has previously been used to test for signs of degradation caused by UV, thermal, and mechanical stress (Cooper and Corcoran 2010, Ojeda et al. 2011). While it is almost certain that UV, heat, and mechanical stresses will work in conjunction with synergistic effects in the marine

environment, studying the impacts of these stresses on their own is a fundamental step in understanding the formation of marine secondary microplastics.

The development of this methodology also highlights the importance of recognizing and controlling contamination, especially by microfibers. Microfibers are omnipresent in the environment and are present in laboratory air and even water (Woodall et al. 2015). Recognizing that these fibers may act as a source of contamination and acting to reduce these fibers is paramount in any methodology aimed at identifying, quantifying or otherwise studying microplastics (Hidalgo-Ruz et al. 2012, Löder and Gerdts 2015, Woodall et al. 2015). The methodology and results presented in this thesis not only establish a replicable testing procedure that can be easily amended to allow additional testing, but also provide a necessary step in understanding the mechanics behind the formation of secondary microplastics. Appreciating mechanisms of microplastic influx into the ocean allows us to better discern the presence of secondary marine microplastics, thus providing a more thorough understanding of exposure and risk which contribute to the development of risk management strategies.

Chapter 3: Methodology

3.1: Experiment 1: UV & Thermal Stress

To test whether plastic degrades and fragments due to UV and heat exposure in a beach environment, virgin PP, LDPE, and HDPE nurdles were exposed to heat stress alone and both UV and heat stress for one year (June 12, 2014 – June 12, 2015).). A nurdle is a small pellet of plastic (not uniform in shape, weighing approximately 0.026g with a volume of 2.7e-8m^3) that serves as the raw material for the manufacturing of plastic products. Furthermore, virgin plastic nurdles were used because they do not contain fillers that impede oxygen diffusion through the material, thus observable physical degradation should be achieved more quickly. Twelve quartz vials were loaded with nurdles of each polymer type (Table 1). Six of these vials (2 of each type of plastic) were covered with white cloth tape to block UV rays and isolate the effects of heat. The other six vials were left for exposure to UV and heat. Additionally, one sample of each polymer type was exposed to neither UV nor extreme temperature (kept at room temperature) for the duration of the experiment to act as a control. The exposed samples were placed in a sandbox in Athens, Georgia (33.95° N, 83.38° W) for 12 months (Appendix A). A WatchDog® weather station that included a micro-station data logger, a UV sensor measuring photon flux density (PFD) over wavelengths from 250 – 400nm (µmol photons/m^2·s), an ambient air temperature and sand-surface temperature sensor was installed on the sandbox to ensure an accurate description of the stresses to which each sample was exposed.

Table 1: Replicates tested for each treatment and polymer type tested

	Polymer Type		
Treatment	**LDPE**	**HDPE**	**PP**
UV and thermal exposure	2	2	2
Thermal exposure	2	2	2
Neither UV or thermal exposure (control)	1	1	1

After the 12 month exposure period, the vials were opened and the nurdles extracted and placed in 20mL scintillation vials. Approximately 10mL of Barnstead™ Nanopure™ filtered water was added (7mL was added directly into the scint vials, and 3mL was first used to rinse the quartz vials before being added to the scint vials).This mixture was poured through US Standard ASTM sieves of sizes 4mm, 2mm, 880µm, and 425µm and the contents visually counted. The sieves were cleaned with an Endecotts sieve brush (for sieves >1mm) or immersed in a bath of Alconox® detergent and water for overnight soaking, then subsequent rinsing and drying, in accordance with ASTM C430 – 96 (ASTM 2009). The solution was filtered through a Whatman 10312609, 2 micron, Grade 602H, 90mm diameter quantitative filter paper circle, and next through a Whatman 10406870 cellulose ME25/21 ST, 47mm white circle with 3.1mm black grid sterile, 0.45 micron mixed ester filter membrane using vacuum filtration. These filters were left for 24 hours to dry before the contents were counted visually using an Olympus SZ40 microscope.

The filtrate that passed through the 0.45µm filter was tested using a Malvern Zetasizer DLS system. This system was in a phase II clean room, which allows a maximum of 10,000 particles per cubic meter for particles ≥0.1µm. A standard operating procedure (SOP) was created to specify the measurement type needed, cell type used, and the material and dispersant properties. In this case, the measurement type was size; the cell type was a DTS0012 – Disposable sizing cuvette; the material was either PP, LDPE, or HDPE with a refractive index and absorption of 1.50 and 0.010, 1.51 and 0.010, and 1.54 and 0.010, respectively (GoodFellow 2015), and the dispersant used was water. The resulting report includes, among other things, a count rate (count rate needs to be between 50 and 300 kilocounts per second (kcps) to ensure an accurate measurement was taken (Wilczura-Wachnik 2005)), a duration used (seconds), a size (nm diameter), a percent intensity, and a standard deviation (nm diameter)(see Appendix B for an example of a full report). Each sample was run three times to ensure accuracy and the resulting peaks combined using the equation 1 to combine sample size (N was

calculated by multiplying the kcps by the duration used, resulting in total kilocount), equation 2 to combine mean (mean (M) is the size in nm diameter), and equation 3 to combine standard deviations for each peak size reported (Berthouex and Brown 2002).

Equation 1: Equation used to combine sample size

$$N_1 + N_2$$

Equation 2: Equation used to combine means

$$\frac{N_1 M_1 + N_2 M_2}{N_1 + N_2}$$

Equation 3: Equation used to combine standard deviations

$$\sqrt{\frac{(N_1 - 1)SD_1^2 + (N_2 - 1)SD_2^2 + \frac{N_1 N_2}{N_1 + N_2}\,(M_1^2 + M_2^2 - 2\,M_1 M_2)}{N_1 + N_2 - 1}}$$

The exposed nurdles were also analyzed with a Nicolet 6700 FTIR system, using ATR-FTIR to test for any signs of oxidation (early signs of degradation) that may not have led to fragmentation. The samples were placed on a germanium crystal and clamped down tightly to ensure contact between the crystal and the sample for accurate measurement. Background spectrums were also measured to provide a relative scale for the absorption intensity. This was done with no sample in the beam and was compared to the measurement taken with the sample to ensure there was no contamination on the crystal and to determine a percent transmittance in the sample. This results in a spectrum which has all of the instrumental or other environmental characteristics removed so that all spectral features present are due strictly to the sample.

The sieving and filtering was performed in a clean fume hood with the negative air on to reduce contamination (Figure 1). Non-plastic lab equipment was used and non-polyester or polyethylene clothing was worn when handling the samples. Additionally, two replicates of 10mL of Barnstead™ Nanopure™ filtered water was passed through the sieves and filtered. The filtrate was tested using DLS,

and the filters examined with the microscope to quantify any contamination in the equipment, air, or water.

Figure 1: Testing area under clean fume hood used to sieve and filter nurdles from experiment 1: UV & thermal stress

To test the hypothesis that exposing plastic to UV and thermal stress will cause degradation and fragmentation, ANOVAs and post hoc Tukey tests were performed on measured changes in weight, sieve counts, and DLS measurements. An ANOVA analyzes group data or procedures to determine if there is a significant difference between them. The Tukey test is performed after the ANOVA and determines which of the measures within a group or procedure are significantly different (Berthouex and Brown 2002). An ANOVA test returns an R^2 value, an F value from a Fisher's F test, and a corresponding probability to the F value, labelled Pr>F. The R^2 value tells what percent of variation in the response variable can be accounted for by the explanatory variables. The F value corresponds to a probability, Pr>F which is the probability that rejecting the null is incorrect. The Tukey test will determine which, if any, of the categories within the explanatory variables are significantly different from one another. Though meticulous steps were taken to reduce contamination, it is inevitable that some amount of contamination, especially by the microfibers present in the air and even water, will

occur (Woodall et al. 2015). These fibers were seen on the filters; to ensure no other factors were affecting the levels of contamination an ANOVA and Tukey test were also performed on the filter fiber counts.

3.2: Experiment 2: Mechanical Stress

To test the hypothesis that mechanical stress causes degradation and fragmentation of PP, virgin PP nurdles were exposed to various treatments for four different time periods (Table 2). PP was chosen because GPC studies LDPE and HDPE under high shear conditions have indicated that most changes in molecular weight distribution occur from thermal or thermo-oxidative degradation, whereas GPC studies of PP indicate production of oxidation products directly as a result of the shear process (Li et al. 2005). Specifically, 500mL of Barnstead™ Nanopure™ filtered water was mixed with ~18.76g of Instant Ocean® (the stoichiometric equivalent of the recommended 1.5lbs/5gal water) in a 2.2L standard toxicity characteristic leaching procedure (TCLP) glass bottle (Figure 2). For half of the treatments 0.25 cups of American Countryside® all-purpose sand (~85g) was also added to the bottles to test the effect of abrasion. Approximately 1.3 g of Bassel Profax 8523 PP nurdles were added to the TCLP bottles, and the bottles placed in an Environmental Express® LE rotator set at 28rpm for 1, 2, 4, or 8 weeks. This rotation creates a mechanical stress exposure similar to what near-shore plastic might experience from wave action in the environment. Before and after exposure the samples were weighed, sieved, filtered, DLS was performed on the filtrate, and ATR-FTIR was performed on the “no sand” exposure nurdles (the sand could scratch the crystal used in ATR-FTIR analyses).

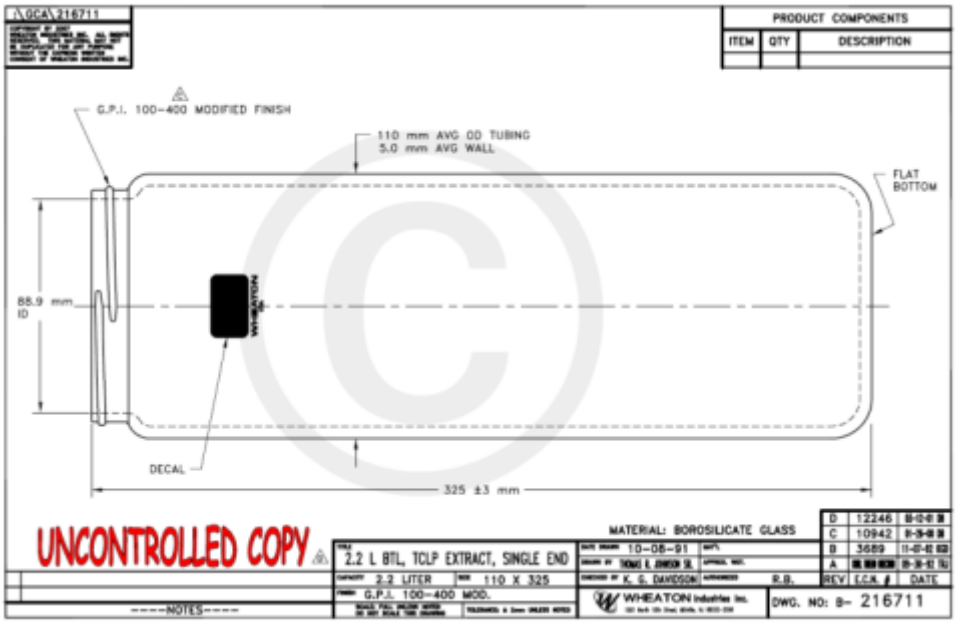

Figure 2: AutoCAD schematic of 2.2L TCLP bottle used in experiment 2: mechanical stress (WHEATON Industries 1992)

Table 2: Replicates tested for each mechanical stress treatment and exposure time

	Exposure Time			
Treatment	**1 week**	**2 weeks**	**4 weeks**	**8 weeks**
Mechanical stress, no sand	2	2	2	2
Mechanical stress, with sand	2	2	2	2
No mechanical stress, no sand	1	1	1	1
No mechanical stress, with sand	1	1	1	1
Mechanical stress, no PP, no sand	2	0	0	0
Mechanical stress, no PP, with sand	2	0	0	0

Before each treatment the PP nurdles, water, Instant Ocean®, and sand (if applicable) were mixed in the TCLP bottles. The contents of the bottles were sieved and filtered as described in experiment 1. The filtrate that passed through the 0.45µm filter was tested using a Malvern Zetasizer DLS system. Similar to experiment 1, the system was in a phase II clean room and an SOP was created. In this case, the measurement type was size; the cell type was a DTS0012 – Disposable sizing cuvette; the material was PP with a refractive index and absorption of 1.50 and 0.010, respectively (GoodFellow 2015), and the dispersant used was water. Again, each sample was run three times and the resulting N,

mean, and standard deviation combined using equations 1, 2, and 3, respectively. After each treatment and exposure period the same methodology was employed.

The filtering and sieving was performed on a clean lab bench (Figure 3). The exposed PP nurdles were kept following exposure, allowed to dry for 24 hours, weighed, and the “no sand” exposure nurdles analyzed with a Nicolet 6700 FTIR system, using ATR-FTIR to look for signs of oxidative degradation. Again, the samples were placed on a germanium crystal and clamped down tightly to ensure accurate measurement, and background spectrums were measured for comparison. A sample of these nurdles was sent to an outside lab (Sea Education Association, Woods Hole, MA) for visual analysis with an AmScope AJX Series Metallurgical microscope using a 5x and occasionally 10x objective with a Schott MLS LED fiber optic sidelight and Lumenera Infinity 2-1RC camera with a 0.5x lens. Image Pro® Premier 9.0 software was used to take pictures, allowing for creation of Z-stacks for Extended Depth of Field.

Figure 3: Testing area on lab bench used to sieve and filter nurdles from experiment 2: mechanical stress

Several controls were used in this experiment. For each treatment and exposure time there was an identical replicate made but not placed in a rotator to experience mechanical stress. There were also 2 replicates each of “sand” and “no sand” TCLP bottles placed in the rotator for 1 week that did not

contain PP nurdles, but were sieved, filtered, and analyzed with DLS after coming out of the rotator. Additionally, Barnstead™ Nanopure™ filtered water was mixed with ~18.76g of Instant Ocean® and this was sieved and filtered, and the filtrate analyzed with DLS. Finally, DLS analysis was performed on Barnstead™ Nanopure™ filtered water poured directly in a scintillation vial to test for contamination of the water itself. Other steps taken to reduce contamination include using non-plastic lab equipment whenever possible and wearing non-polyester or polyethylene clothing when handling the samples.

To test the hypothesis that following mechanical stress and/or abrasion PP will degrade and fragment, ANOVAs and Tukey tests were performed on the percent change in pre- and post- treatment weight and sieve count, as well as percent intensity in a given range for the DLS measurements. The Malvern Zetasizer system output report specifies three distinct peaks present in the sample (see Appendix B for an example of a full report). In a majority of the reports for this experiment, only one peak was reported which fell within the 100-1,000nm diameter range, thus this is the range that was tested for any significant changes. Though steps were taken to reduce contamination, numerous fibers were found on the filters. To ensure that this contamination was independent of the various treatments and exposure times, ANOVAs and Tukey tests were also performed on fiber counts.

Chapter 4: Results & Discussion

4.1: Experiment 1: UV & Thermal Stress

PP, LDPE, and HDPE were exposed to thermal only and UV and thermal stress in a controlled beach environment. Because sand has a lower specific heat than air (664J/kg·˚C versus ~1,000J/kg·˚C) the sand will heat and cool more quickly and to a greater extent than the air. For example, on the hottest day recorded, the sand reached a temperature of 123.9 ^{o}F while the ambient air temperature was 98.2 ^{o}F. Similarly, on the coldest day recorded, the sand's surface was 6.3^{o}F while the air was 11.7^{o}F (Figure 4). The temperature throughout the year (June 12, 2014 to June 12, 2015) for both the sand surface and ambient air was roughly evenly distributed, with 60-70^{o}F being the most common temperature (Figure 5). The PFD from 250-400nm measured by the WatchDog® weather station showed extreme differences between PFD in the summer versus winter (Figure 6), but the average throughout the year was similar to NREL's solar radiation annual average maps for the region (NREL 2015). The total photon flux was over 914 moles photons/m^2; therefore the ~1.5m^2 sandbox absorbed a total of 1,371 mols photons. For one nurdle of volume ~2.7e-8m^3 and half a surface area of ~5.4e-6m^2, this is approximately 4,900 µmols of photons striking each nurdle over the course of the year.

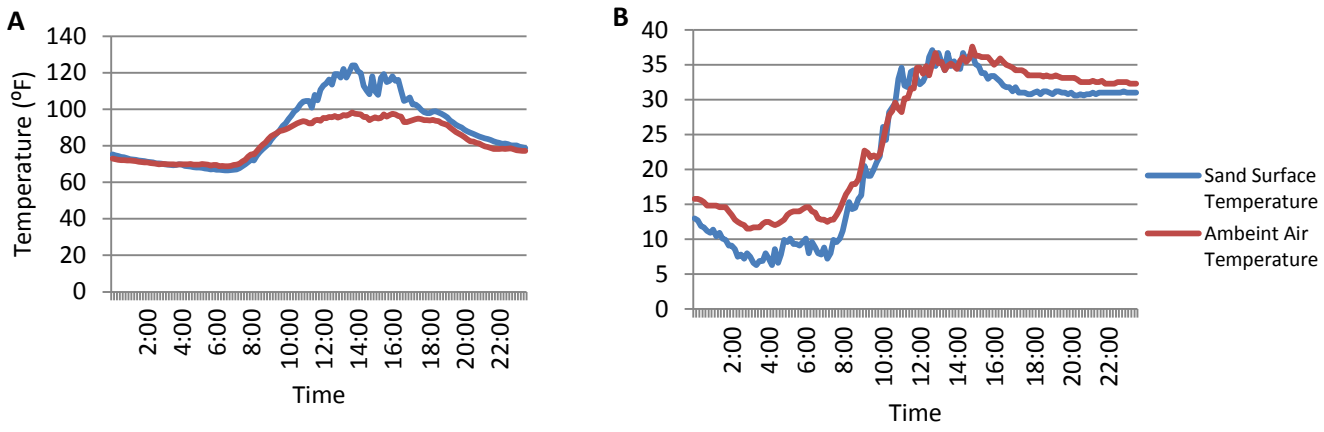

Figure 4: Temperature of sand surface and ambient air for the hottest (A) and coldest (B) days recorded at the test site from June 2014 - June 2015

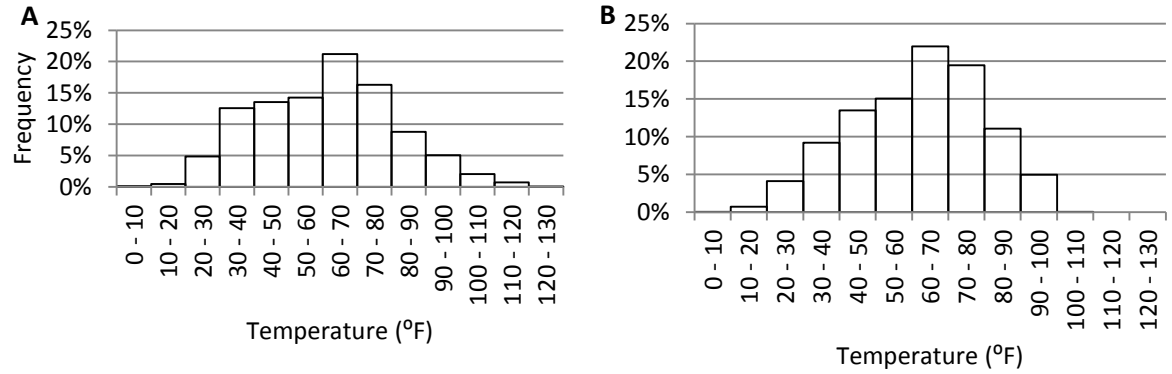

Figure 5: Frequency of temperatures recorded for sand surface (A) and ambient air (B) at the test site from June 2014 - June 2015

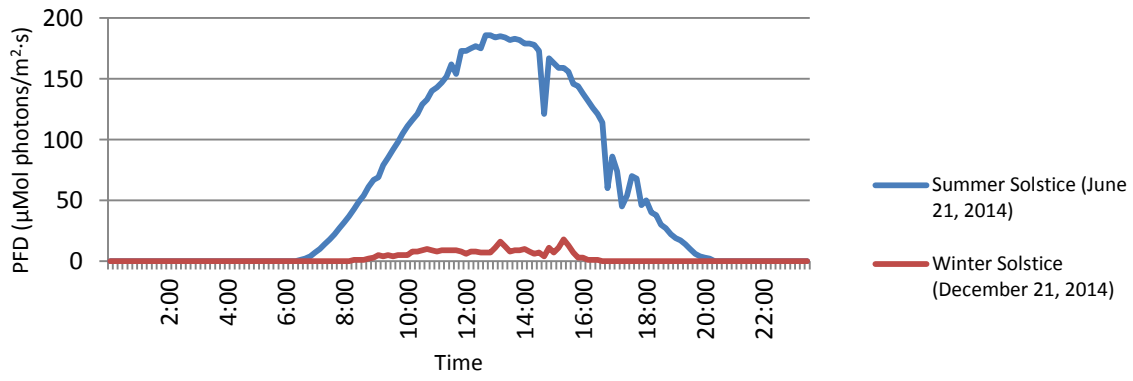

Figure 6: PFD recorded on the summer solstice (June 21, 2014) and the winter solstice (December 21, 2014) at the test site

The response variables tested in the ANOVA and Tukey tests for weight was specific weight per nurdle (total weight divided by total count); for sieve count the response variable tested was percent count in the 2 mm sieve (nurdles were only found in the 4 and 2 mm sieves so this is the count found in 2mm sieve divided by total count); for DLS the response variable was percent intensity detected in the 50 – 500 nm diameter range (the most common range detected in this experiment, see Figure 7 for an example DLS output) and for the contamination tests the response variable tested was the fiber count. The mean, standard deviation, and 95% confidence interval for each of these variables is in Table 3 and a list of the raw data is in Appendix C. The response and explanatory variables, along with the explanatory variable categories tested in each ANOVA and Tukey are listed in Table 4. Table 5 summarizes the results of the ANOVA and Tukey test for each of the response variables tested.

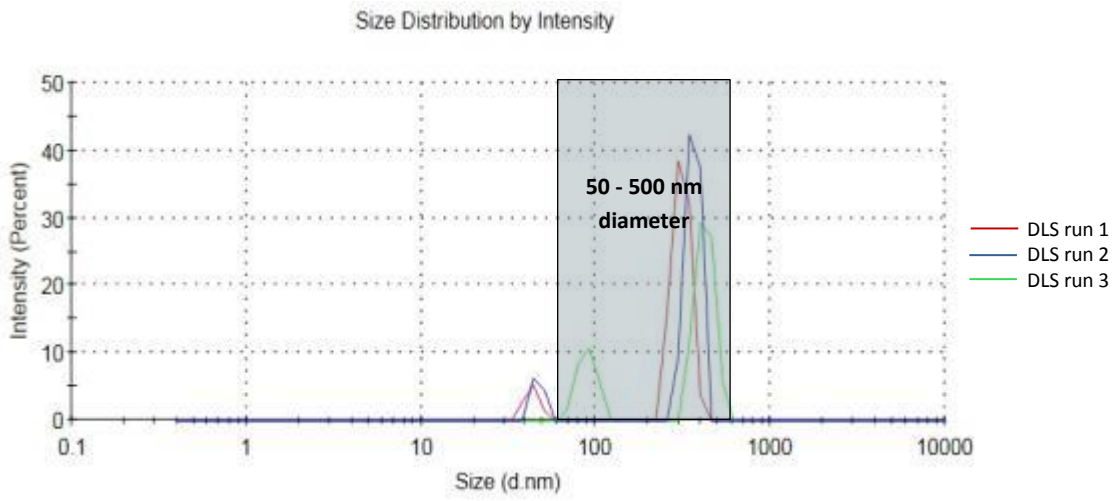

Figure 7: DLS results of testing HDPE thermal exposure only treatment; size distribution by intensity is reported and the 50 - 500nm diameter range shown

Table 3: Summary table of mean, standard deviation, and 95% confidence interval for each variable tested

Variable	n	Mean	Standard Deviation	95% Confidence Interval
Weight/nurdle	15	0.026	0.0058	0.0029
% count in 2 mm sieve	15	75.5%	33.9%	17.2%
DLS % intensity detected in 50-500nm diameter range	17	98.7%	3.79%	1.80%
2 µm filter				
Clear fiber count	17	1.70	0.79	0.37
Colored fiber count	17	1.00	0.79	0.38
0.45µm filter				
Clear fiber count	17	11.6	3.84	1.83
Colored fiber count	17	1.12	0.93	0.44

Table 4: Response variable and explanatory variables and their categories analyzed in ANOVA and Tukey tests

	Response variable	Explanatory variables	Categories
Test 1	Weight/nurdle	Polymer type	PP, LDPE, HDPE
		Treatment	UV & thermal, thermal only, neither
Test 2	Percent count in 2mm sieve	Polymer type	PP, LDPE, HDPE
		Treatment	UV & thermal, thermal only, neither
Test 3	Percent intensity in 50 – 500 nm diameter range	Polymer type	PP, LDPE, HDPE
		Treatment	UV & thermal, thermal only, neither, N/A (contamination controls)
Test 4	Fiber count	Polymer type	PP, LDPE, HDPE
		Treatment	UV & thermal, thermal only, neither, N/A (contamination controls)
		Fiber color	Colored or clear
		Filter	2 µm or 0.45 µm

Table 5: Summary table of selected results from the ANOVA and Tukey tests of each response variable

		ANOVA			Tukey test
	Response Variable	**R^2**	**Pr > F**	**Explanatory variables**	**Significant Differences**
Test 1	Weight/nurdle	99.4%	< 0.01%	Polymer type	Significant differences between PP, LDPE, and HDPE
				Treatment	No significant differences
Test 2	Percent count in 2mm sieve	99.9%	> 0.01%	Polymer type	Significant difference between LDPE and PP and HDPE
				Treatment	No significant differences
Test 3	Percent intensity in 50 – 500 nm diameter range	32.1%	44.3%	Polymer type	No significant differences
				Treatment	No significant differences
Test 4	Fiber count	60.1%	< 0.01%	Polymer type	No significant differences
				Treatment	No significant differences
				Fiber color	Significant difference between colored and clear fiber count
				Filter	Significant difference between 2µm and 0.45µm filters

The results show that variation in both the weight/nurdle and percent count in 2mm sieve response variables are highly accounted for by the explanatory variables and there is less than a 0.01% probability that the null hypothesis (no effect of the explanatory variables) is correct. However, the Tukey test reveals that since there are no significant differences between the treatments, it is the polymer type that is responsible for these effects. As different polymers will have different manufacturing processes and therefore the nurdles will have different sizes and weights from the outset, this is logical. For example, regardless of treatment, the average nurdle weight for PP, LDPE, and HDPE was 0.020g ± 6.9e-4g, 0.034g ± 4.8e-4g, and 0.025g ± 9.0e-5g, respectively. The ANOVA also showed that a majority of the variation in percent intensity in the 50 – 500nm diameter range could not be accounted for and that there is a high probability that rejecting the null hypothesis would be incorrect. Additionally, there were no significant differences between polymer type or treatment to account for the variation in percent intensity in the 50 – 500 nm diameter range. Finally, while the R^2 value for fiber count was low compared to Tests 1 and 2, the Pr > F shows that there is less than 0.01% probability that the null is correct. The categories of polymer type and treatment had no significant

differences detected, but fiber color and filter categories did. This makes sense; regardless of treatment, polymer type, or filter type, the average count for colored and clear fibers was 1.1 ± 0.85 and 6.6 ± 5.8, respectively. Similarly, regardless of treatment, polymer type, or fiber color the average fiber count on 2µm and 0.45µm filters was 1.3 ± 0.84 and 6.4 ± 6.0, respectively. While it seems that there were more clear fibers present and also more fibers captured by the 0.45µm filter, the polymer type and treatments did not have an effect. See Figure 8 for examples of fibers found during this experiment.

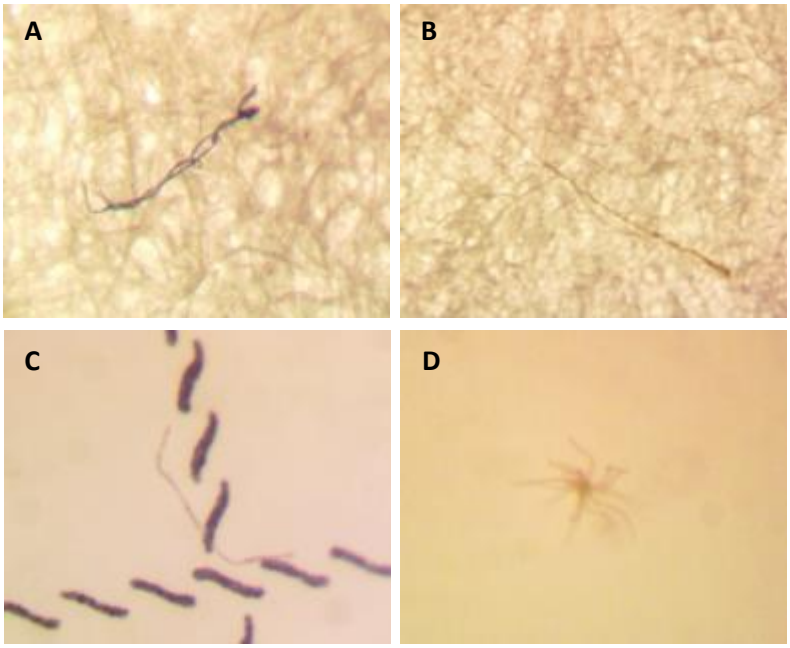

Figure 8: Example of fibers counted on 2µm and 0.45µm filters in experiment 1. (A) Blue fiber on 2µm filter; (B) clear fiber on 2µm filter; (C) clear fiber on 0.45µm filter; (D) clear 'star' fiber on 0.45µm filter

To test for signs of degradation that did not yet progress to the extent of fragmentation the exposed nurdles were analyzed using ATR-FTIR to look for signs of oxidation (Figure 9). In each figure below, the nurdle exposed to UV and thermal stress has a greater absorbance and broader band area in the carbonyl peak range (1640-1840cm^{-1}) than either the thermal exposure or no exposure nurdles. Additionally, the LDPE and PP thermal exposure carbonyl peak absorbance and area are greater than seen with no exposure. This indicates that the exposed nurdles did undergo oxidative degradation to a greater extent than the nurdles not exposed. Though weight and size distribution tests did not reveal

any changes that would suggest fragmentation, the time frame and exposures were sufficient to initiate and propagate the degradation process through some oxidation of the polyolefin chain. Furthermore this shows that UV and thermal stresses together will generally degrade plastic more quickly and to a greater extent than thermal stress alone. In these results the approximate ratios between the maximum absorbance in the carbonyl peak region for UV and thermal exposure:No exposure and Thermal exposure:No exposure is shown in Table 6. Though HDPE has a higher ratio of maximum absorbance for UV & thermal exposure:No exposure than LDPE, PP has a higher ratio than HDPE, and both PP and LDPE have higher ratio of Thermal exposure:No exposure than does HDPE. It has previously been shown that both PP and LDPE will degrade more quickly than HDPE (Chiellini et al. 2006, Ojeda et al. 2011) The complete spectra for HDPE, LDPE, and PP are shown in Appendix D.

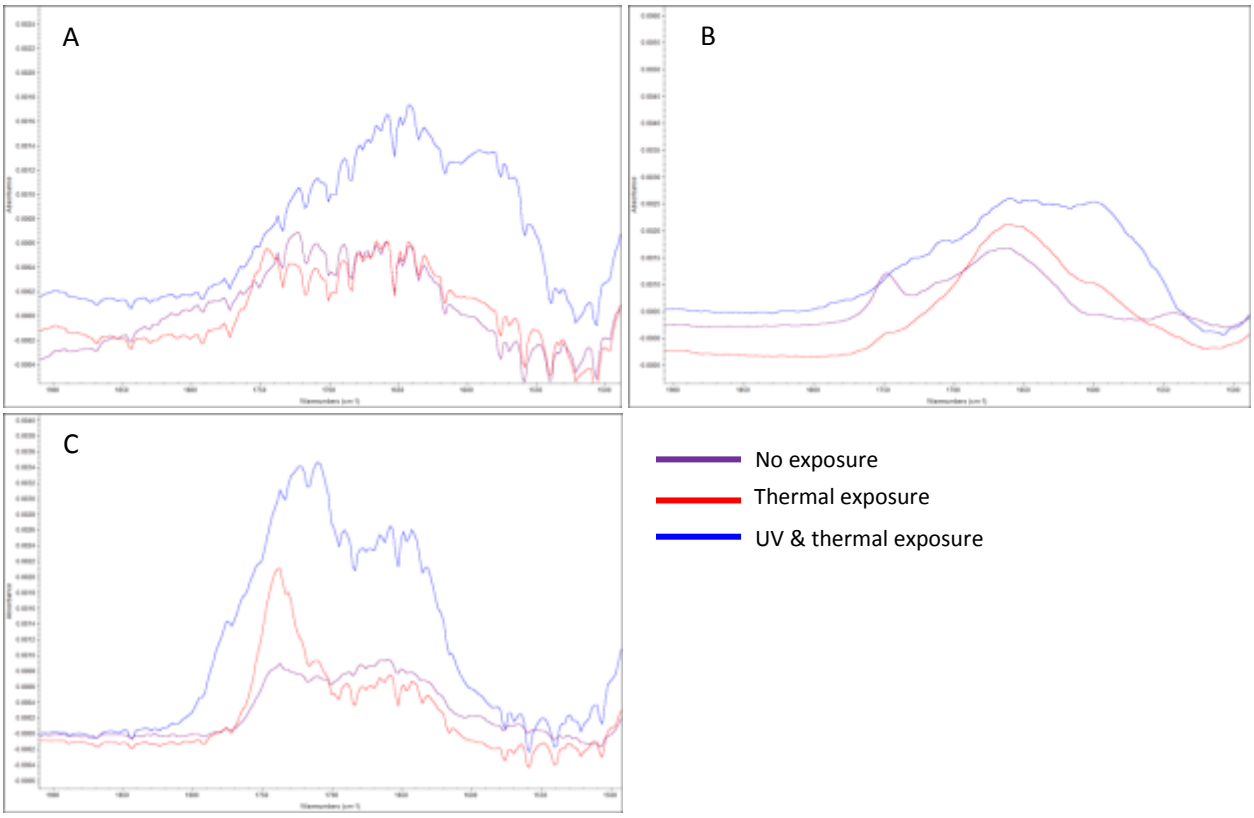

Figure 9: ATR-FTIR sprectra in absorption band 1640-1840 cm^{-1} (carbonyl peak) for (A) HDPE; (B) LDPE; (C) PP

Table 6: Approximate ratios between maximum absorbance in the carbonyl peak region for no exposure, thermal exposure, and UV & thermal exposure, and the resulting ratios

Polymer Type	**Maximum Absorbance**			**Ratio of Maximum Absorbance**	
	No exposure	*Thermal exposure*	*UV & thermal exposure*	*Thermal exposure:No exposure*	*UV & thermal exposure:No exposure*
HDPE	0.0006	0.0006	0.0018	1	3
LDPE	0.0015	0.002	0.0025	1.33	1.67
PP	0.0008	0.0022	0.0036	2.75	4.5

4.2: Experiment 2: Mechanical Stress

As stated in the Methods, samples of virgin PP were placed in a rotator set at 28rpm or left to sit (no mechanical abrasion) for 1, 2, 4, and 8 weeks. Several assumptions were made in order to calculate the force to which each nurdle was exposed. These assumptions include the following: nurdles are spherical, nurdles are fully submerged (equal hydrostatic pressure), momentum comes to zero at each half-turn of the rotator, and centrifugal force was neglected. Based on a total weight of contents in the 2.2L bottles of approximately 605g, a travelling distance (Δx) of 244.45mm (see Figure 2), a travelling time (Δt) of 1.06s, and a nurdle surface area of approximately 4.36e-5m^2, we calculated the total weekly force on each nurdle to be approximately 5,500N. Waves are created from an energy transfer between wind and the ocean surface, and since wind speed and direction are constantly shifting wave action is considered a random process and is thus hard to replicate (Ochi 2005). However, from a study of the force of breaking waves on intertidal organisms coupled with the average surface area of these organisms (Lowell 1984, Denny 1985), we calculated that one of our plastic nurdles would experience between 4,100 – 4,800N of force in a week from breaking waves. These numbers are very close, especially considering the vast variability in wave action and force.

To test for fragmentation and contamination, both ANOVA and post-hoc Tukey tests were performed on the response variables: percent change (from pre- to post-treatment) of weight and count in the 2mm sieve (nurdles were only found in the 4 and 2 mm sieves), percent intensity detected in the

100-1,000 nm diameter range (the most common range detected, see Figure 10 for an example of DLS output), and for fiber count on the filters. The mean, standard deviation, and 95% confidence interval for each response variable is in Table 7 and a table of the raw data is in Appendix E. These response variables along with their respective explanatory variables and categories tested are in Table 8. Table 9 summarizes the results of the test for each of the response variables tested, including an R^2 value and a Pr>F value from the ANOVA and which, if any, of the categories within the explanatory variables are significantly different from each other from the Tukey test.

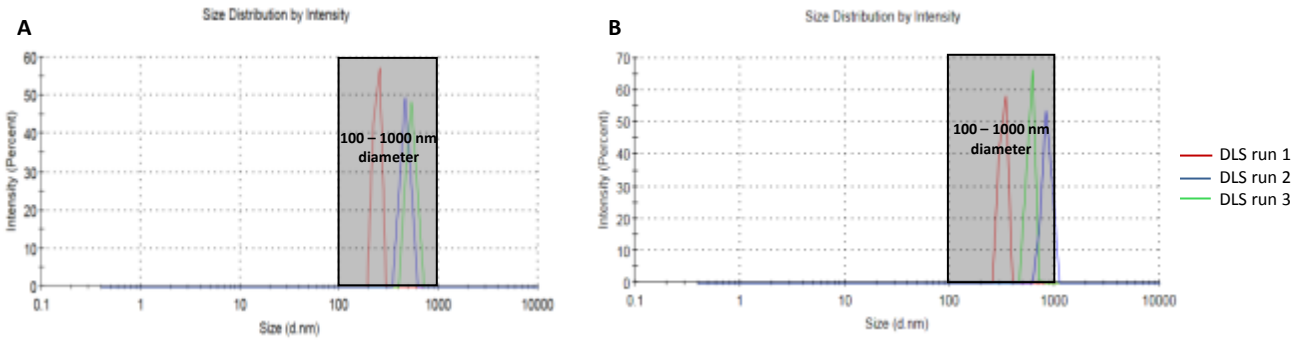

Figure 10: Output from Malvern DLS system with 100-1,000 diameter range shown for (A) pre- and (B) post- 8 week, no sand, mechanical stress treatment

Table 7: Table of mean, standard deviation, and 95% confidence interval for each variable tested

Variable	n	Mean	Standard Deviation	95% Confidence Interval
% change in total weight of nurdles	24	0.77%	2.12%	0.85%
% change in count in 2mm sieve	24	7.0%	12.4%	4.9%
DLS % intensity detected in 100-1,000nm diameter range				
Pre-treatment	25	87.6%	25.3%	9.9%
Post-treatment	30	92.2%	14.6%	5.2%
2µm filter				
Pre-treatment				
Clear fiber count	29	11.38	6.44	2.35
Colored fiber count	29	7.93	4.28	1.56
Post-treatment				
Clear fiber count	28	10.89	5.61	2.08
Colored fiber count	28	6.96	3.42	1.27
0.45µm filter				
Pre-treatment				
Clear fiber count	29	18.41	13.95	5.08
Colored fiber count	29	6.41	3.60	1.31
Post-treatment				
Clear fiber count	28	16.71	11.37	4.21
Colored fiber count	28	6.82	3.98	1.47

Table 8: Response variable and explanatory variables and categories analyzed in ANOVA and Tukey tests

	Response variable	Explanatory variables	Categories
Test 1	Percent change in weight	Exposure time	1, 2, 4, or 8 weeks
		Treatment	Mechanical stress with sand, mechanical stress with sand, no mechanical stress no sand, no mechanical stress with sand
Test 2	Percent change in count in 2mm sieve	Exposure time	1, 2, 4, or 8 weeks
		Treatment	Mechanical stress with sand, mechanical stress with sand, no mechanical stress no sand, no mechanical stress with sand
Test 3	Percent intensity in 100 – 1,000 nm diameter range	Exposure time	1, 2, 4, or 8 weeks, N/A (contamination control)
		Treatment	Mechanical stress no sand, mechanical stress with sand, no mechanical stress no sand, no mechanical stress with sand, N/A (contamination control)
		Stage	Pre or post treatment
Test 4	Fiber count	Fiber color	Colored or clear
		Exposure time	1, 2, 4, or 8 weeks, N/A (contamination control)
		Treatment	Mechanical stress no sand, mechanical stress with sand, no mechanical stress no sand, no mechanical stress with sand, N/A (contamination control)
		Filter	2 µm or 0.45 µm
		Stage	Pre or post treatment

Table 9: Summary table of selected results from the ANOVA and Tukey tests of each response variable analyzed

		ANOVA			Tukey test
	Response Variable	**R^2**	**Pr > F**	**Explanatory variables**	**Significant Differences**
Test 1	Percent change in weight	35.8%	21.4%	Exposure time	No significant differences
				Treatment	No significant differences
Test 2	Percent change in count in 2mm sieve	38.8%	16.0%	Exposure time	No significant differences
				Treatment	No significant differences
Test 3	Percent intensity in 100 – 1000 nm diameter range	10.1%	87.6%	Exposure time	No significant differences
				Treatment	No significant differences
				Stage	No significant differences
Test 4	Fiber count	25.6%	<0.01%	Exposure time	No significant differences
				Treatment	No significant differences
				Fiber color	Significant difference between count of colored and clear fibers
				Filter	Significant difference between 2µm and 0.45µm filters
				Stage	No significant differences

The results show that only 35.8% of variation in percent change in weight can be accounted for by the explanatory variables, and a Pr>F of 21.4% indicates that there is a 21.4% probability that rejecting the null hypothesis (that there is no effect of explanatory variables on the response variable) is incorrect. Generally, this should be at least 5% for the null to be rejected with 95% confidence. Additionally, the Tukey test revealed that there were no significant differences between exposure time or treatment. Similarly, the ANOVA returned an R^2 of 38.8% for Test 2 and 10.1% for Test 3, the Pr>F was too high to reject the null in either test, and there were no significant differences in exposure times or treatment in Test 2 or significant differences in exposure time, treatment, or stage for Test 3. This indicates that based on the parameters measured, mechanical stress has no effect. This finding is reinforced by the Sea Education Association, Woods Hole, MA outside lab analysis of the nurdles post-treatment. Through examination of the nurdles with a high-powered microscope, it was concluded that the samples looked similar to new nurdles, regardless of exposure time or treatment. The nurdles from the "sand" treatment did appear rougher, but it is likely that this was due to sand stuck to the surface

(see Figure 11 for example pictures). Perhaps this is not surprising; tests of cyclic loading rates until failure for virgin PP use similar loading frequencies (0.5 Hz = 30 rpm) but the stresses and cycles to failure are both multiple orders of magnitude greater than the stresses and cycles to which we exposed the PP nurdles (Maier and Calafut 1998). Furthermore, these cyclic loading rate tests only examine the material until the point of failure; however, embrittlement and subsequent fragmentation occur after mechanical failure has been reached (Andrady 2015). Thus the cycles to embrittlement and amount of stress needed to induce embrittlement will be greater than those needed for causing mechanical failure alone.

In Test 4, the ANOVA returned an R^2 of 25.6% and the Pr>F is such that the null can be rejected with greater than 99.9% confidence. The Tukey test revealed that among the explanatory variables, there were significant differences between the categories for fiber color and filter. This is logical; regardless of treatment, exposure time, filter, or stage, the average count on each filter for colored and clear fibers was 6.9 ± 3.8 and 14.3 ± 10.2, respectively. Similarly, regardless of exposure time, treatment, fiber color, or stage, the average fiber count for 2µm and 0.45µm filters was 9.4 ± 5.7 and 12.6 ± 10.8, respectively. While there were more clear fibers present and also more fibers captured by the 0.45µm filter, the polymer type and treatments did not have an effect. See Figure 12 for examples of fibers found during this experiment.

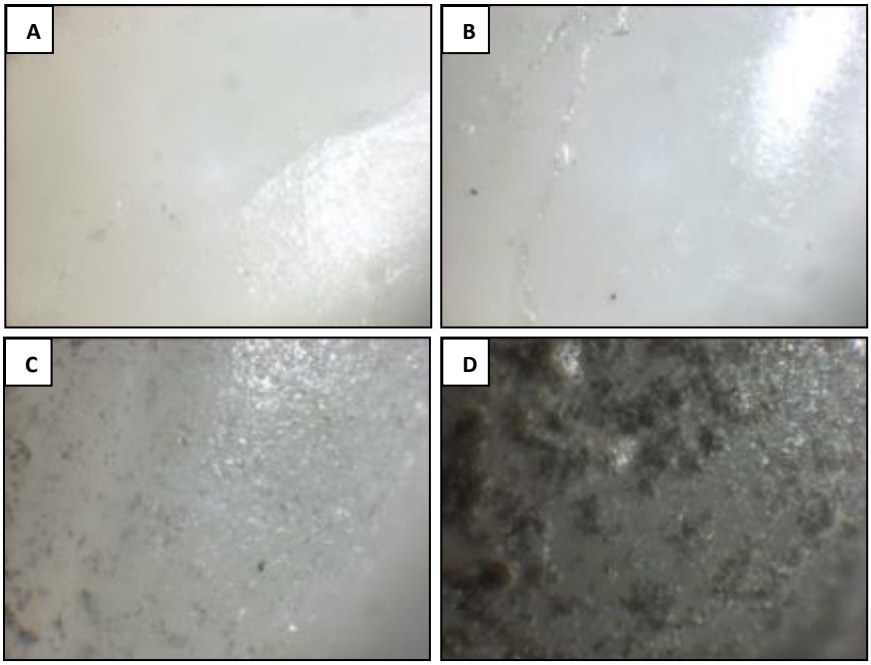

Figure 11: Example pictures taken with and Lumenera Infinity 2-1RC camera of nurdle surfaces post-treatment. (A) 8 weeks, no mechanical stress, no sand; (B) 8 weeks, mechanical stress, no sand; (C) 1 week, mechanical stress, with sand; (D) 8 weeks, mechanical stress, with sand

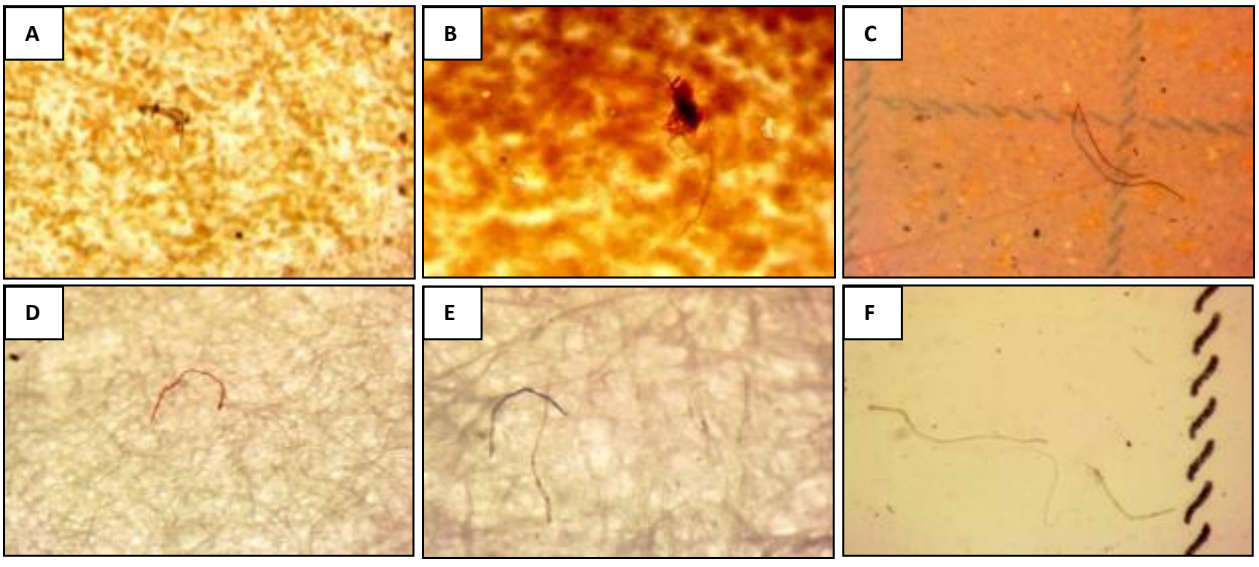

Figure 12: Example of fibers seen on 2µm and 0.45µm filters in experiment 2. (A) clear fiber on 2µm filter after filtering a pre-treatment, 1 week, no mechanical stress, with sand sample; (B) red fiber on 2µm filter after filtering a post-treatment, 1 week, mechanical stress, no plastic, with sand sample; (C) black fiber on 0.45µm filter after filtering a pre-treatment, 8 week, no mechanical stress, with sand sample; (D) red fiber on 2µm filter after filtering a pre -treatment, 2 week, mechanical stress, no sand sample; (E) black and clear fiber on 2µm filter after filtering a post-treatment, 1 week, no mechanical stress, no sand sample; (F) multiple clear fibers on 0.45µm filter after filtering a post-treatment, 4 week, mechanical stress, no sand sample

To test for signs of degradation that did not yet progress to the extent of fragmentation the exposed nurdles were analyzed using ATR-FTIR to look for signs of oxidation (Figure 13). Though both post 1 and 8 week exposures have greater absorbance than the no exposure nurdle, the no mechanical stress and mechanical stress absorbance and band area are roughly equal. This indicates that though some oxidation process is taking place it is not the effects of mechanical stress that is producing these larger peaks. The complete spectra for post 1 week and 8 week treatments are shown in Appendix F.

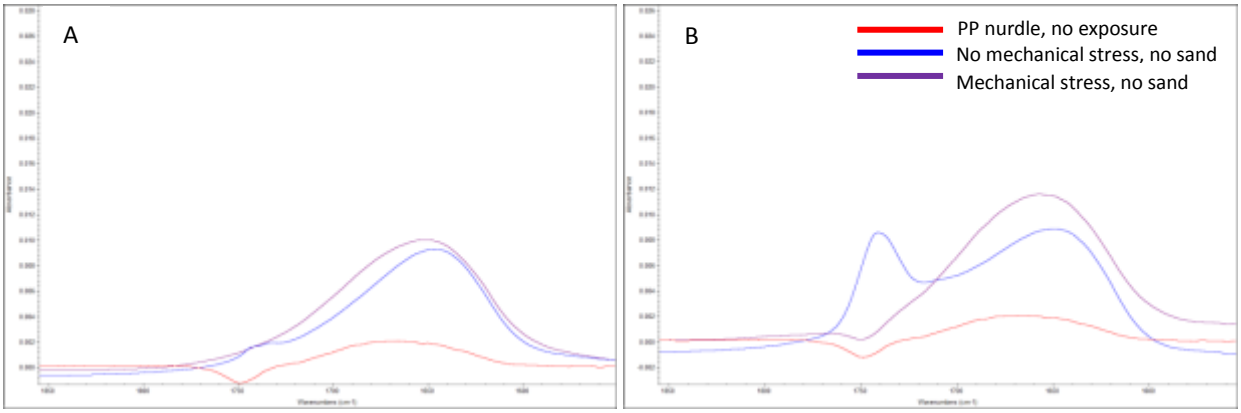

Figure 13: ATR-FTIR sprectra in absorption band 1640-1840 cm-1 (carbonyl peak) for (A) post 1 week exposure and (B) post 8 week exposure

Chapter 5: Future Recommendations

5.1: Additional testing for degradation and fragmentation

These experiments did not demonstrate evidence of fragmentation. Because fragmentation only occurs after sufficient weathering and subsequent embrittlement (Andrady 2015) this indicates that the exposure periods, levels of UV, thermal, and mechanical stress, or both, used in these experiments were not sufficient. For further exploration we suggest that UV, thermal, and mechanical stresses be used together. This will almost certainly increase the speed and extent of degradation and subsequent fragmentation. As seen in Figure 9, the UV and thermal exposures caused oxidation in the plastics. Once degradation has been initiated it is reasonable to expect mechanical stress and abrasion to then slough off this top layer of degraded plastic, thus resulting in fragmented pieces (Barnes et al. 2009, Andrady 2015). To test this theory, the HDPE, LDPE, and PP nurdles that have now been exposed to thermal only and UV and thermal stresses for one year, and have demonstrated at least some level of oxidation, can undergo mechanical stress and abrasion similar to that performed in experiment 2. To further increase the rate and extent of degradation and fragmentation it may also be beneficial to use thin film plastics as oppose to nurdles. Since these degradation processes generally occur as surface phenomenon (Singh and Sharma 2008), larger surface area to volume ratios will likely result in faster degradation and subsequent fragmentation.

Because we did not find indications of fragmentation does not necessarily mean that the stresses did not induce changes. The ATR-FTIR results demonstrate that the LDPE, HDPE, and PP nurdles did undergo some level of oxidation due to UV and thermal stresses. The mechanical stress treatments also demonstrated signs of oxidation greater than those nurdles with no treatment, however it cannot be said that this oxidation is due to the mechanical stress and abrasion. These results revealed that

some chemical changes were occurring, and additional chemical changes may be revealed through tests such as using size exclusion chromatography to determine changes in molar mass distribution or using differential scanning calorimetry analysis to determine changes in second melting or crystallization temperatures or degree of crystallinity (Ojeda et al. 2011). Additionally, for the mechanical stress exposures in particular, scanning electron microscopy could reveal surface cracks or pitting that could not be seen with the microscope. When testing degradation of plastic material scientists generally look at the mechanical properties of plastic, but rarely test plastic degraded beyond the point of mechanical failure. Though embrittlement and fragmentation will occur after this point (Andrady 2015), similar to testing the chemical properties of the plastic, mechanical properties testing may offer some insight into the initial degradation and embrittlement process. These mechanical tests could include looking for changes in impact resistance, impact fatigue, brittleness, stress-strain relationships or tensile or compressive strength.

5.2: Recommendations for contamination control

Though our methodology was designed to minimize contamination, numerous fibers were still present. For instance, the analyses in experiment 2 were actually performed before the analyses for experiment 1, and in experiment 2 we did not yet realize the extent of contamination. Compare Figure 3 to Figure 1, for example: experiment 2 was performed on the lab bench while experiment 1 was performed under a clean fume hood with the negative air on. This reduced the total fiber count on filters from 17.9 ± 6.6 (post-treatment average fiber count) to 2.6 ± 0.9 in the 2µm filter and from 23.5 ± 13.0 (post-treatment average fiber count) to 12.8 ± 4.1 in the 0.45µm filter. Still, additional steps could have been taken to potentially reduce these contamination levels further. Ideally, all of the analyses would have been performed in a phase I clean room, which allows a maximum of 10 particles per cubic meter for particles ≥0.1µm (International Organization for Standardization 1999). However, working in a

clean room may not be feasible, so there are several simple contamination mitigation strategies that may be employed in the lab. These include covering all vents with a natural fiber cloth, deep cleaning all surfaces, adding a filter to the water supply, wearing natural fiber clothing to cover body and hair, and limiting access to the processing laboratory (Woodall et al. 2015). Still it is not likely that these strategies will reduce the contamination levels to zero. Thus it is important to know the baseline levels of contamination in the lab. In our experiments we did this through extensive use of controls testing water, air, and lab equipment for contamination. It is also important to note that looking for contamination on filters using a microscope can be very subjective. To ensure consistent results either a single person should be responsible for conducting all of the fiber counts, or at least if there are multiple people they should be similarly trained. Finally, though not necessary for our experiments, some testing of microplastics may require that the contamination fibers be identified. To do this, methods such as Raman spectroscopy or FTIR could be employed. It is also important to note that if these tests are being performed on the filter or filtrate directly that a background must be taken that includes the filtrate solution or filter being used. This will allow a subtraction of background spectra from sample spectra, revealing possibly minute peaks associated with the contamination.

Chapter 6: Conclusions

Plastic use has essentially become compulsory in human society; while some of these plastics are durable and designed for long-term use, a large portion are used once and then thrown away. Inevitably some fraction of this plastic waste will be mismanaged, and some fraction of that mismanaged waste will enter the ocean. Longevity of marine plastic debris is reported to be between hundreds and thousands of years, and this process is likely even slower at depth (Barnes et al. 2009). However, there is evidence that through UV, heat, and mechanical stress plastics do become weathered and brittle enough to fragment and form microplastics (Thompson et al. 2004). Plastic debris in the ocean and microplastics in particular present a multitude of negative environmental impacts. A substantial barrier to a greater understanding of microplastic quantity and dispersion is the absence of a standard methodology (Hidalgo-Ruz et al. 2012, Löder and Gerdts 2015). This is further complicated by the ubiquity of microplastic contamination, particularly microfibers, in the environment and in the lab (Woodall et al. 2015). Before any management strategy can be designed and enacted, a deeper understanding of the ecological risks and exposure levels must be gleaned. This means establishing standard methodologies for identifying and quantifying microplastics, and also a more fundamental understanding of the formation of these microplastics.

The aim of this study was to establish and test a replicable, widely applicable methodology to analyze marine microplastic. We also provide a more fundamental understanding of the formation of microplastics by examining the effects of the most prominent stresses in the marine environment on plastic. While both studies show null results with respect to fragmentation we were able to demonstrate signs of oxidative degradation. Therefore both studies provide an indication of the extent and timescale of plastic degradation and fragmentation due to specific, known levels of stress. This establishes an

initial threshold; as we know the precise environment and stress that each sample was exposed, and we know that those stresses did not elicit a change in the response variables tested, these studies may act as a benchmark for additional studies. Not only is it likely that these environmental stresses acting together will accelerate fragmentation in the response variables tested, but it is also suspected that testing of other response variables will demonstrate additional changes on a microscopic chemical and/or physical level. Additionally, we demonstrated the importance of considering contamination in any study looking at microplastics, and discuss steps to both mitigate and establish baseline levels of this contamination in any testing space.

Based on increasing global population and plastic production, microplastic abundance in the ocean is expected to rise; however comprehensive understanding of future trends in quantity and dispersion of this micropollutant is still limited. Even so, there seems to be a global consensus that reducing marine plastic debris is in the best interest of both the environment and human population. Before effective mitigation or management strategies can be developed we need to further our understanding of the scope of the problem. We know that upon entering the ocean some plastics will degrade and fragment; we do not know the rate or extent of this fragmentation nor do we have an extensive knowledge of the ecological impacts of the resulting microplastics. To facilitate progress in the study of plastic fragmentation we developed a methodology for testing the formation of microplastics and provide a benchmark for studying secondary microplastic production in the marine environment.

References

American Meteorological Society. 2012. Meteorology Glossary: hydroperoxyl radical.*in* A. M. Society, editor.

Andrady, A. 2015. Persistence of Plastic Litter in the Oceans.*in* M. Bergmann, L. Gutow, and M. Klages, editors. Marine anthropogenic litter. Springer, Berlin.

Andrady, A., J. Pegram, and Y. Tropsha. 1993. Changes in carbonyl index and average molecular weight on embrittlement of enhanced-photodegradable polyethylenes. Journal of environmental polymer degradation **1**:171-179.

Andrady, A. L. 1990. Weathering of polyethylene (LDPE) and enhanced photodegradable polyethylene in the marine environment. Journal of Applied Polymer Science **39**:363-370.

Andrady, A. L. 2011. Microplastics in the marine environment. Marine Pollution Bulletin **62**:1596-1605.

Arther, C., J. Baker, and H. E. Bamford. 2008. Proceedings of the International Research Workshop on the Occurrence, Effects, and Fate of Microplastic Marine Debris.*in* International Research Workshop on the Occurrence, Effects, and Fate of Microplastic Marine Debris. NOAA Technical Memoradum NOS-OR&R-30, University of Washington Tacoma, Tacoma, WA.

ASTM. 2009. ASTM Standard C430-96. Standard Test Method for Fineness of Hydraulic Cement by the 45-µm (No. 325) Sieve, West Conshohocken, PA, 2009.

Barnes, D. K., F. Galgani, R. C. Thompson, and M. Barlaz. 2009. Accumulation and fragmentation of plastic debris in global environments. Philosophical Transactions of the Royal Society B: Biological Sciences **364**:1985-1998.

Berne, B. J. and R. Pecora. 2000. Dynamic light scattering: with applications to chemistry, biology, and physics. Courier Corporation.

Berthouex, P. M. and L. C. Brown. 2002. Statistics for Environmental Engineers. Lewis Publishers, Boca Raton, FL.

Besseling, E., A. Wegner, E. M. Foekema, M. J. van den Heuvel-Greve, and A. A. Koelmans. 2012. Effects of microplastic on fitness and PCB bioaccumulation by the lugworm Arenicola marina (L.). Environmental Science & Technology **47**:593-600.

Browne, M. A., A. Dissanayake, T. S. Galloway, D. M. Lowe, and R. C. Thompson. 2008. Ingested microscopic plastic translocates to the circulatory system of the mussel, Mytilus edulis (L.). Environmental Science & Technology **42**:5026-5031.

Browne, M. A., T. S. Galloway, and R. C. Thompson. 2010. Spatial patterns of plastic debris along estuarine shorelines. Environmental Science & Technology **44**:3404-3409.

Chiellini, E., A. Corti, S. D'antone, and R. Baciu. 2006. Oxo-biodegradable carbon backbone polymers–oxidative degradation of polyethylene under accelerated test conditions. Polymer Degradation and Stability **91**:2739-2747.

Cooper, D. A. and P. L. Corcoran. 2010. Effects of mechanical and chemical processes on the degradation of plastic beach debris on the island of Kauai, Hawaii. Marine Pollution Bulletin **60**:650-654.

Corcoran, P. L., M. C. Biesinger, and M. Grifi. 2009. Plastics and beaches: A degrading relationship. Marine Pollution Bulletin **58**:80-84.

Cózar, A., F. Echevarría, J. I. González-Gordillo, X. Irigoien, B. Úbeda, S. Hernández-León, Á. T. Palma, S. Navarro, J. García-de-Lomas, and A. Ruiz. 2014. Plastic debris in the open ocean. Proceedings of the National Academy of Sciences **111**:10239-10244.

Denny, M. W. 1985. Wave forces on intertidal organisms: A case study. Limnology and Oceanography **30**:1171-1187.

Derraik, J. G. 2002. The pollution of the marine environment by plastic debris: a review. Marine Pollution Bulletin **44**:842-852.

do Sul, J. A. I., Â. Spengler, and M. F. Costa. 2009. Here, there and everywhere. Small plastic fragments and pellets on beaches of Fernando de Noronha (Equatorial Western Atlantic). Marine Pollution Bulletin **58**:1236-1238.

Engler, R. E. 2012. The complex interaction between marine debris and toxic chemicals in the ocean. Environmental Science & Technology **46**:12302-12315.

Eriksen, M., L. C. Lebreton, H. S. Carson, M. Thiel, C. J. Moore, J. C. Borerro, F. Galgani, P. G. Ryan, and J. Reisser. 2014. Plastic pollution in the world's oceans: more than 5 trillion plastic pieces weighing over 250,000 tons afloat at sea. PloS one **9**:e111913.

GoodFellow. 2015. Material Information.*in* I. Goodfellow, editor.

Gregory, M. R. 2009. Environmental implications of plastic debris in marine settings—entanglement, ingestion, smothering, hangers-on, hitch-hiking and alien invasions. Philosophical Transactions of the Royal Society B: Biological Sciences **364**:2013-2025.

Hidalgo-Ruz, V., L. Gutow, R. C. Thompson, and M. Thiel. 2012. Microplastics in the marine environment: a review of the methods used for identification and quantification. Environmental Science & Technology **46**:3060-3075.

Hitchings, L. 2014. Why Illinois has banned exfoliating face washes. NewScientist. Reed Business Information Ltd.

Hoornweg, D. and Bhada-Tata. 2012. What a waste: A global review of solid waste managment. The World Bank, Washington DC.

International Organization for Standardization. 1999. Cleanrooms and associated controlled environments Part 1 : Classification of air cleanliness.

Jambeck, J. R., R. Geyer, C. Wilcox, T. R. Siegler, M. Perryman, A. Andrady, R. Narayan, and K. L. Law. 2015. Plastic waste inputs from land into the ocean. Science **347**:768-771.

Kato, H., M. Suzuki, K. Fujita, M. Horie, S. Endoh, Y. Yoshida, H. Iwahashi, K. Takahashi, A. Nakamura, and S. Kinugasa. 2009. Reliable size determination of nanoparticles using dynamic light scattering method for in vitro toxicology assessment. Toxicology in Vitro **23**:927-934.

Kühn, S., E. L. Bravo Rebolledo, and J. A. van Franeker. 2015. Deleterious Effects of Litter of Marine Life.*in* M. Bergmann, L. Gutow, and M. Klages, editors. Marine anthropogenic litter. Springer, Berlin.

Law, K. L., S. Morét-Ferguson, N. A. Maximenko, G. Proskurowski, E. E. Peacock, J. Hafner, and C. M. Reddy. 2010. Plastic accumulation in the North Atlantic subtropical gyre. Science **329**:1185-1188.

Li, Y., J. Li, S. Guo, and H. Li. 2005. Mechanochemical degradation kinetics of high-density polyethylene melt and its mechanism in the presence of ultrasonic irradiation. Ultrasonics sonochemistry **12**:183-189.

Löder, M. G. J. and G. Gerdts. 2015. Methodology Used for the Detection and Identification of Microplastics - A Critical Appraisal. Pages 201-227 *in* M. Bergmann, L. Gutow, and M. Klages, editors. Marine anthropogenic litter. Springer, Berlin.

Lowell, R. 1984. Desiccation of intertidal limpets: effects of shell size, fit to substratum, and shape. Journal of Experimental Marine Biology and Ecology **77**:197-207.

Maier, C. and T. Calafut. 1998. Polypropylene: The Definitive User's Guide and Databook. Plastics Design Library, Norwich NY.

Malvern Instuments. 2004. Zetasizer Nano Series User Manual. Worcestershire, UK.

Martinez, E., K. Maamaatuaiahutapu, and V. Taillandier. 2009. Floating marine debris surface drift: convergence and accumulation toward the South Pacific subtropical gyre. Marine Pollution Bulletin **58**:1347-1355.

Mato, Y., T. Isobe, H. Takada, H. Kanehiro, C. Ohtake, and T. Kaminuma. 2001. Plastic resin pellets as a transport medium for toxic chemicals in the marine environment. Environmental Science & Technology **35**:318-324.

Murdock, R. C., L. Braydich-Stolle, A. M. Schrand, J. J. Schlager, and S. M. Hussain. 2008. Characterization of nanomaterial dispersion in solution prior to in vitro exposure using dynamic light scattering technique. Toxicological Sciences **101**:239-253.

NREL. 2015. Dynamic Maps, GIS Data, & Analysis Tools. PV Solar Radiation Static Maps. National Renewable Energy Laboratory.

Obbard, R. W., S. Sadri, Y. Q. Wong, A. A. Khitun, I. Baker, and R. C. Thompson. 2014. Global warming releases microplastic legacy frozen in Arctic Sea ice. Earth's Future **2**:315-320.

Ochi, M. K. 2005. Ocean waves: the stochastic approach. Cambridge University Press.

Ojeda, T., A. Freitas, K. Birck, E. Dalmolin, R. Jacques, F. Bento, and F. Camargo. 2011. Degradability of linear polyolefins under natural weathering. Polymer Degradation and Stability **96**:703-707.

PerkinElmer. 2005. FT-IR Spectroscopy: Attenuated Total Reflectance (ATR). PerkinElmer Life and Analytical Sciences, Shelton, CT.

Pham, C. K., E. Ramirez-Llodra, C. H. Alt, T. Amaro, M. Bergmann, M. Canals, J. Davies, G. Duineveld, F. Galgani, and K. L. Howell. 2014. Marine litter distribution and density in European seas, from the shelves to deep basins.

PlasticsEurope. 2014. Plastics - the Facts 2014. PlasticsEurope, Brussels, Belgium.

Rochman, C. M. 2015. The Complex Mixture, Fate and Toxicity of Chemicals Associated with Plastic Debris in the Marine Environment.*in* M. Bergmann, L. Gutow, and M. Klages, editors. Marine anthropogenic litter. Springer, Berlin.

Rochman, C. M., E. Hoh, T. Kurobe, and S. J. Teh. 2013. Ingested plastic transfers hazardous chemicals to fish and induces hepatic stress. Scientific reports **3**.

Rochman, C. M., T. Kurobe, I. Flores, and S. J. Teh. 2014. Early warning signs of endocrine disruption in adult fish from the ingestion of polyethylene with and without sorbed chemical pollutants from the marine environment. Science of the Total Environment **493**:656-661.

Singh, B. and N. Sharma. 2008. Mechanistic implications of plastic degradation. Polymer Degradation and Stability **93**:561-584.

Syberg, K., F. R. Khan, H. Selck, A. Palmqvist, G. T. Banta, J. Daley, L. Sano, and M. B. Duhaime. 2015. Microplastics: addressing ecological risk through lessons learned. Environmental Toxicology and Chemistry **34**:945-953.

Teuten, E. L., S. J. Rowland, T. S. Galloway, and R. C. Thompson. 2007. Potential for plastics to transport hydrophobic contaminants. Environmental Science & Technology **41**:7759-7764.

Thermo Nicolet. 2001. Introduction to Fourier Transform Infrared Spectroscopy. Thermo Nicolet Corporation.

Thompson, R. C., Y. Olsen, R. P. Mitchell, A. Davis, S. J. Rowland, A. W. John, D. McGonigle, and A. E. Russell. 2004. Lost at sea: where is all the plastic? Science **304**:838-838.

Timmers, M. A., C. A. Kistner, and M. J. Donohue. 2005. Marine Debris of the Northwestern Hawaiian Islands: Ghost Net Identification. US Department of Commerce, National Oceanic and Atmospheric Administration, National Sea Grant College Program.

Van Cauwenberghe, L., A. Vanreusel, J. Mees, and C. R. Janssen. 2013. Microplastic pollution in deep-sea sediments. Environmental pollution **182**:495-499.

Watson, R., C. Revenga, and Y. Kura. 2006. Fishing gear associated with global marine catches: I. Database development. Fisheries Research **79**:97-102.

WHEATON Industries, I. 1992. Uncontrolled Copy: 2.2 L BTL, TCLP Extract, Single End.*in* D. N. B-216711, editor.

Wilczura-Wachnik, H. 2005. Manual for experiment: Dynamic Light Scattering application in size detection of molecules and molecular aggregates.

Woodall, L. C., C. Gwinnett, M. Packer, R. C. Thompson, L. F. Robinson, and G. L. Paterson. 2015. Using a forensic science approach to minimize environmental contamination and to identify microfibres in marine sediments. Marine Pollution Bulletin.

Woodall, L. C., A. Sanchez-Vidal, M. Canals, G. L. Paterson, R. Coppock, V. Sleight, A. Calafat, A. D. Rogers, B. E. Narayanaswamy, and R. C. Thompson. 2014. The deep sea is a major sink for microplastic debris. Royal Society Open Science **1**:140317.

Ye, S. and A. L. Andrady. 1991. Fouling of floating plastic debris under Biscayne Bay exposure conditions. Marine Pollution Bulletin **22**:608-613.

Appendix A

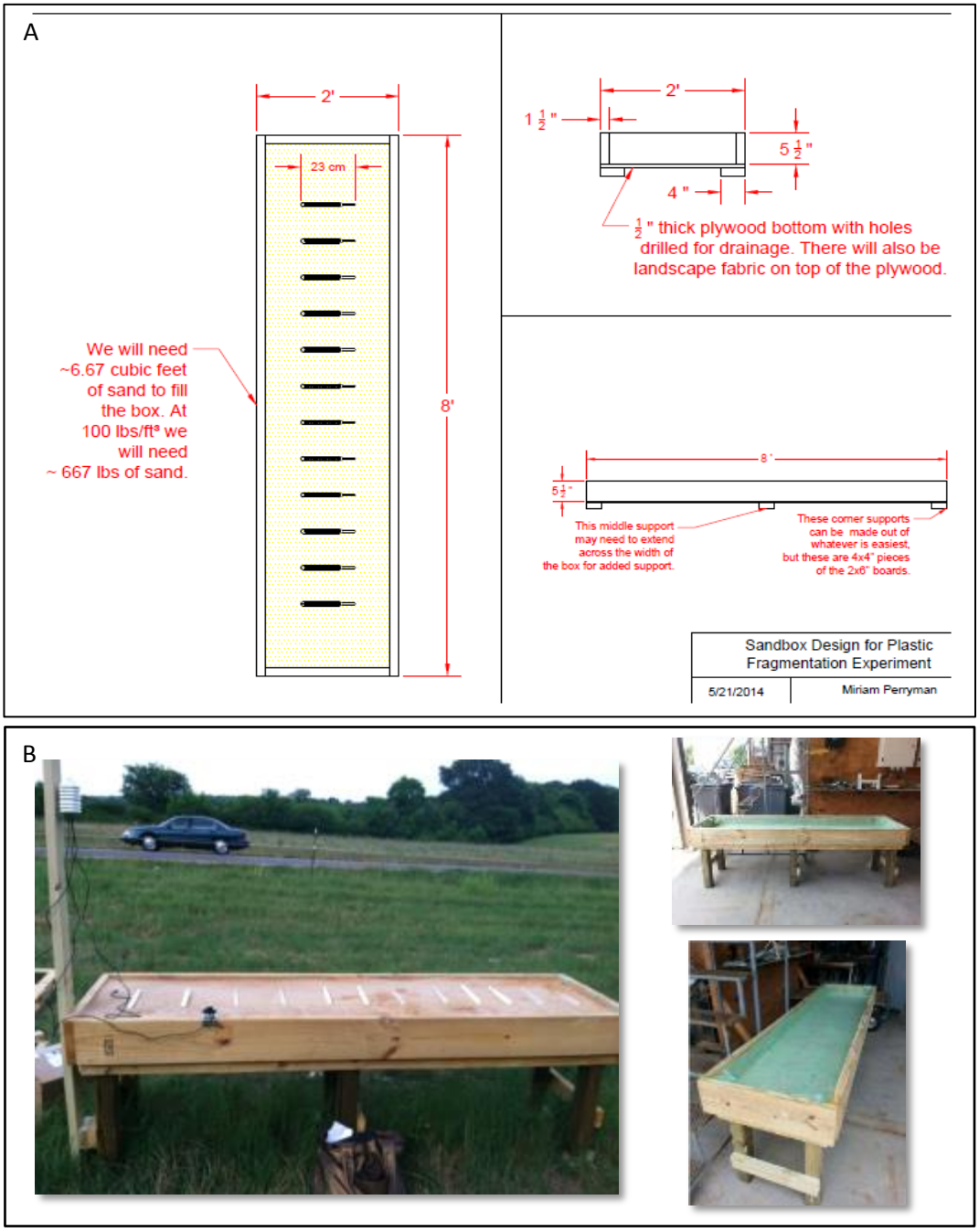

Figure 14: Sandbox used in experiment 1: UV & thermal stress. (A) schematic of sandbox; (B) pictures of final product

Appendix B

Size Distribution Report by Intensity

v2.2

Malvern

Sample Details

Sample Name:	Sample3cs3.25_Triall1_5.25_ 1		
SOP Name:	PP_3.31_2		
General Notes:			
File Name:	Installation tests.dts	**Dispersant Name:**	Water
Record Number:	178	**Dispersant RI:**	1.330
Material RI:	1.50	**Viscosity (cP):**	0.8872
Material Absorbtion:	0.010	**Measurement Date and Time:**	Monday, May 25, 2015 11:18:...

System

Temperature (°C):	25.0	**Duration Used (s):**	60
Count Rate (kcps):	222.8	**Measurement Position (mm):**	4.65
Cell Description:	Disposable sizing cuvette	**Attenuator:**	10

Results

			Size (d.nm):	% Intensity:	St Dev (d.n...
Z-Average (d.nm):	2538	**Peak 1:**	211.1	100.0	13.79
PdI:	1.000	**Peak 2:**	0.000	0.0	0.000
Intercept:	0.648	**Peak 3:**	0.000	0.0	0.000

Result quality : Refer to quality report

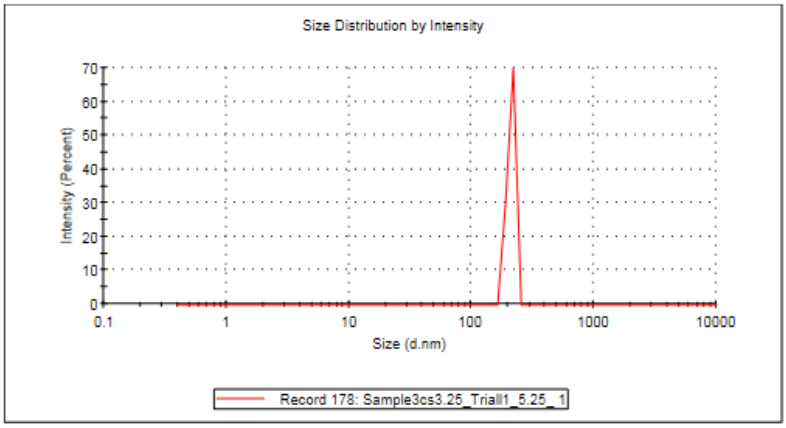

Figure 15: Malvern Zetasizer dynamic light scattering output reporting size distribution by intensity for 8 week, post mechanical treatment with sand, trial 1

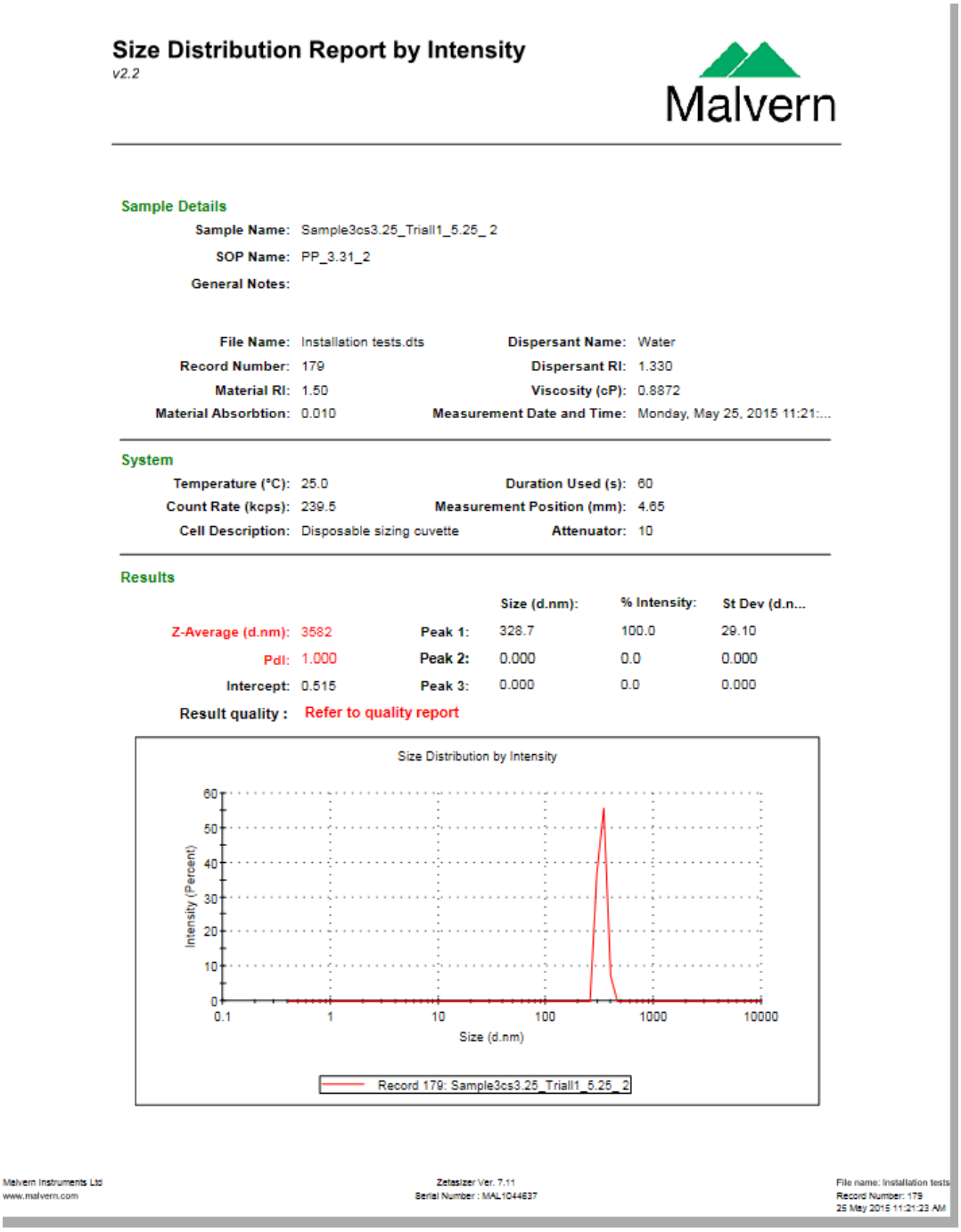

Size Distribution Report by Intensity

v2.2

Malvern

Sample Details

Sample Name:	Sample3cs3.25_Triall1_5.25_ 2		
SOP Name:	PP_3.31_2		
General Notes:			
File Name:	Installation tests.dts	**Dispersant Name:**	Water
Record Number:	179	**Dispersant RI:**	1.330
Material RI:	1.50	**Viscosity (cP):**	0.8872
Material Absorbtion:	0.010	**Measurement Date and Time:**	Monday, May 25, 2015 11:21:...

System

Temperature (°C):	25.0	**Duration Used (s):**	60
Count Rate (kcps):	239.5	**Measurement Position (mm):**	4.65
Cell Description:	Disposable sizing cuvette	**Attenuator:**	10

Results

			Size (d.nm):	% Intensity:	St Dev (d.n...
Z-Average (d.nm):	3582	**Peak 1:**	328.7	100.0	29.10
PdI:	1.000	**Peak 2:**	0.000	0.0	0.000
Intercept:	0.515	**Peak 3:**	0.000	0.0	0.000

Result quality : Refer to quality report

Figure 16: Malvern Zetasizer dynamic light scattering output reporting size distribution by intensity for 8 week, post mechanical treatment with sand, trial 2

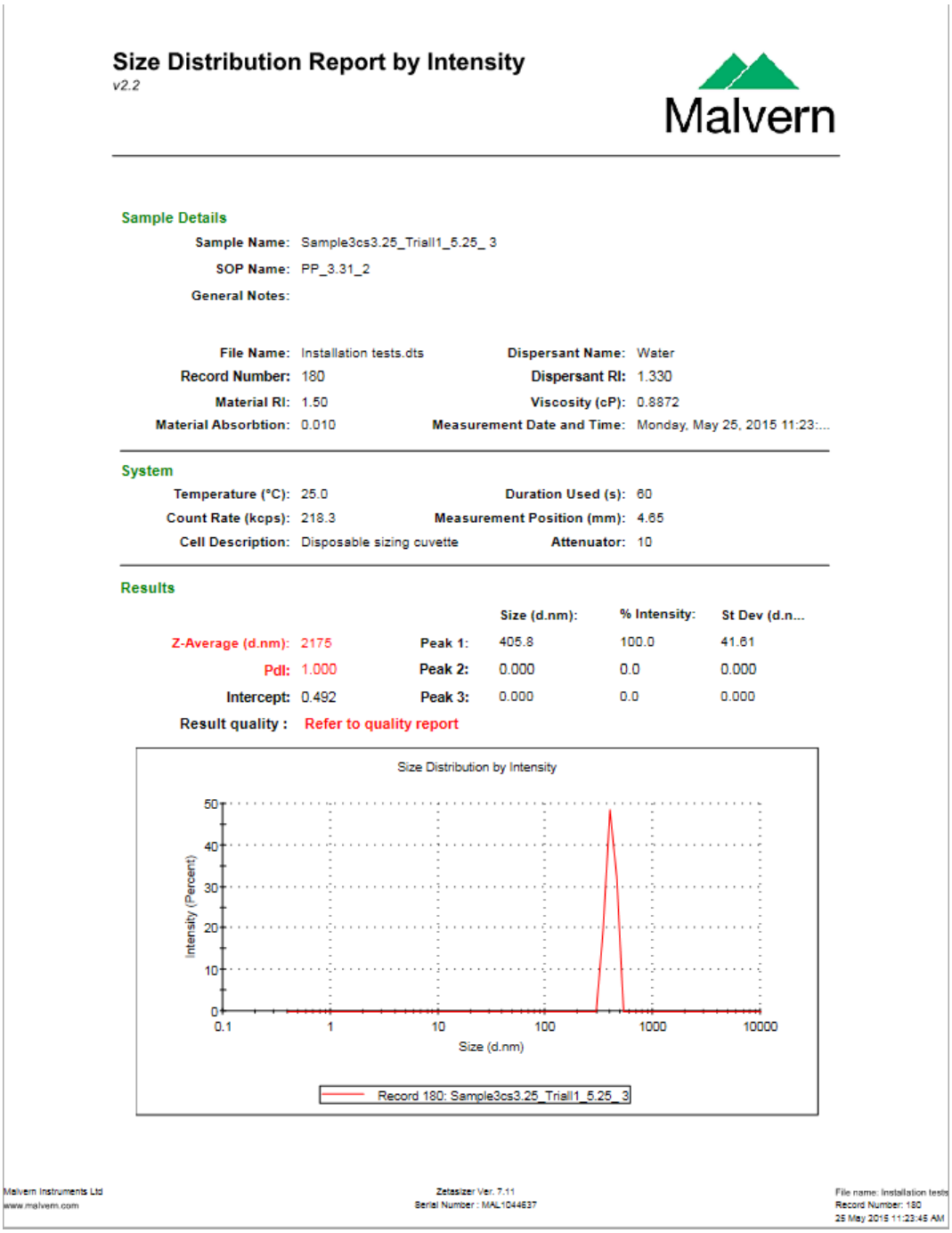

Size Distribution Report by Intensity

v2.2

Malvern

Sample Details

Sample Name:	Sample3cs3.25_Triall1_5.25_ 3		
SOP Name:	PP_3.31_2		
General Notes:			
File Name:	Installation tests.dts	**Dispersant Name:**	Water
Record Number:	180	**Dispersant RI:**	1.330
Material RI:	1.50	**Viscosity (cP):**	0.8872
Material Absorbtion:	0.010	**Measurement Date and Time:**	Monday, May 25, 2015 11:23:...

System

Temperature (°C):	25.0	**Duration Used (s):**	60
Count Rate (kcps):	218.3	**Measurement Position (mm):**	4.65
Cell Description:	Disposable sizing cuvette	**Attenuator:**	10

Results

			Size (d.nm):	% Intensity:	St Dev (d.n...
Z-Average (d.nm):	2175	**Peak 1:**	405.8	100.0	41.61
PdI:	1.000	**Peak 2:**	0.000	0.0	0.000
Intercept:	0.492	**Peak 3:**	0.000	0.0	0.000

Result quality : Refer to quality report

Figure 17: Malvern Zetasizer dynamic light scattering output reporting size distribution by intensity for 8 week, post mechanical treatment with sand, trial 3

Size Distribution Report by Intensity

v2.2

Malvern

Sample Details

Sample Name:	Sample3cs3.25_Triall1_5.25_ 3		
SOP Name:	PP_3.31_2		
General Notes:			
File Name:	Installation tests.dts	**Dispersant Name:**	Water
Record Number:	180	**Dispersant RI:**	1.330
Material RI:	1.50	**Viscosity (cP):**	0.8872
Material Absorbtion:	0.010	**Measurement Date and Time:**	Monday, May 25, 2015 11:23:...

System

Temperature (°C):	25.0	**Duration Used (s):**	60
Count Rate (kcps):	218.3	**Measurement Position (mm):**	4.65
Cell Description:	Disposable sizing cuvette	**Attenuator:**	10

Results

			Size (d.nm):	% Intensity:	St Dev (d.n...
Z-Average (d.nm):	2175	**Peak 1:**	405.8	100.0	41.61
PdI:	1.000	**Peak 2:**	0.000	0.0	0.000
Intercept:	0.492	**Peak 3:**	0.000	0.0	0.000

Result quality : Refer to quality report

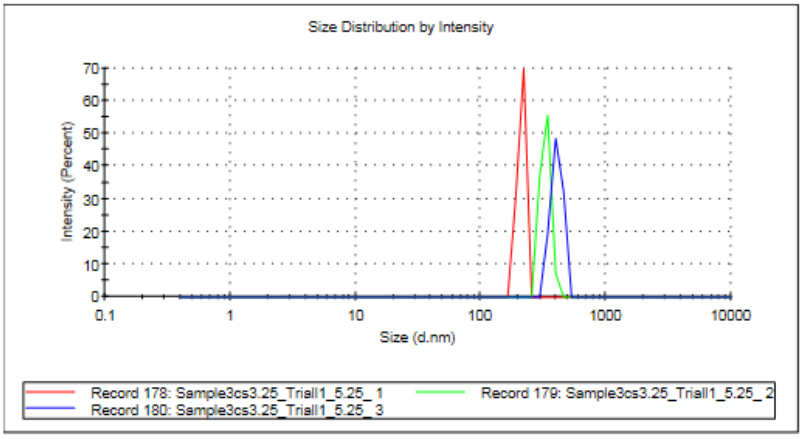

Figure 18: Malvern Zetasizer dynamic light scattering output reporting size distribution by intensity for 8 week, post mechanical treatment with sand, trial 1-3 combined

Appendix C

Table 10: Raw data for experiment 1: UV & thermal stress of weight, sieve count, and fiber count

Name	Description	Weight	Sieve Count		Avg Nurdle Wt	2 micron filter		0.45 micron filter	
			4 mm	2 mm		Clear	Colored	Clear	Colored
Vial 1 (L2)	LDPE, UV & Therm	1.5984	34	13	0.03401	1	3	11	3
Vial 2 (L4)	LDPE, UV & Therm A	1.8797	42	13	0.03418	3	1	11	0
Vial 3 (L1)	LDPE, Therm only	1.9302	40	18	0.03328	1	1	7	1
Vial 11 (L3)	LDPE, Therm only A	1.8094	39	15	0.03351	2	0	11	2
Vial 5 (H3)	HDPE, UV & Therm	2.3344	0	93	0.02510	3	1	10	1
Vial 6 (H4)	HDPE, UV & Therm A	2.1695	0	87	0.02494	2	0	20	2
Vial 7 (H1)	HDPE, Therm only	2.2664	0	91	0.02491	2	1	11	1
Vial 8 (H2)	HDPE, Therm only A	2.1491	0	86	0.02499	1	0	12	0
Vial 9 (P4)	PP, UV & Therm	1.9755	1	95	0.02058	2	1	8	1
Vial 10 (P3)	PP, UV & Therm A	2.2327	2	112	0.01959	1	1	15	1
Vial 4 (P1)	PP, Therm only	2.0067	0	104	0.01930	3	1	10	0
Vial 12 (P2)	PP, Therm only A	2.0826	0	100	0.02083	1	2	11	0
Con1	Control, water sieved and filtered	n/a	n/a	n/a	n/a	2	0	9	1
Con2	Control 2, water sieved and filtered	n/a	n/a	n/a	n/a	1	1	7	2
PP Control	PP, No Treatment	5.4763	6	260	0.02059	1	1	15	0
LDPE Control	LDPE, No Treatment	4.228	92	36	0.03303	1	1	20	2
HDPE Control	HDPE, No Treatment	5.1236	0	206	0.02487	1	2	10	2
	Average:	2.6175	17.07	88.60	0.03	1.65	1.00	11.65	1.12
	Standard deviation:	1.242068	26.96	70.08	0.01	0.79	0.79	3.84	0.93
	95% confidence interval:	0.628561	13.64	35.46	0.00	0.37	0.38	1.83	0.44

Table 11: Raw data for experiment 1: UV & thermal stress for DLS

	50-500nm diameter range			0-50nm diameter range		
Name	Average Peak (nm) (combined)	% Intensity (combined)	Standard Deviation (nm) (combined)	Average Peak (nm) (combined)	% Intensity (combined)	Standard Deviation (nm) (combined)
Vial 1 (L2)	194.88	100%	55.17			
Vial 2 (L4)	114.44	100%	74.49			
Vial 3 (L1)	212.7	100%	56.56			
Vial 11 (L3)	219.16	100%	27			
Vial 5 (H3)	137.37	100%	56.66			
Vial 6 (H4)	96.29	100%	31.37			
Vial 7 (H1)	73.3	100%	29.19			
Vial 8 (H2)	363.19	84.60%	61.11	49.22	15.60%	21.77
Vial 9 (P4)	240.84	100%	59.03			
Vial 10 (P3)	244.38	100%	54.35			
Vial 4 (P1)	98.53	100%	64.66			
Vial 12 (P2)	171.92	97.67%	63.88	9.95	2.33%	17.64
Con1	276.15	100%	135.15			
Con2	111.55	100%	65.17			
PP Control	178.97	100%	79.99			
LDPE Control	258.83	100%	77.24			
HDPE Control	241.44	96.27%	106.24	25.82	3.73%	20.43

Appendix D

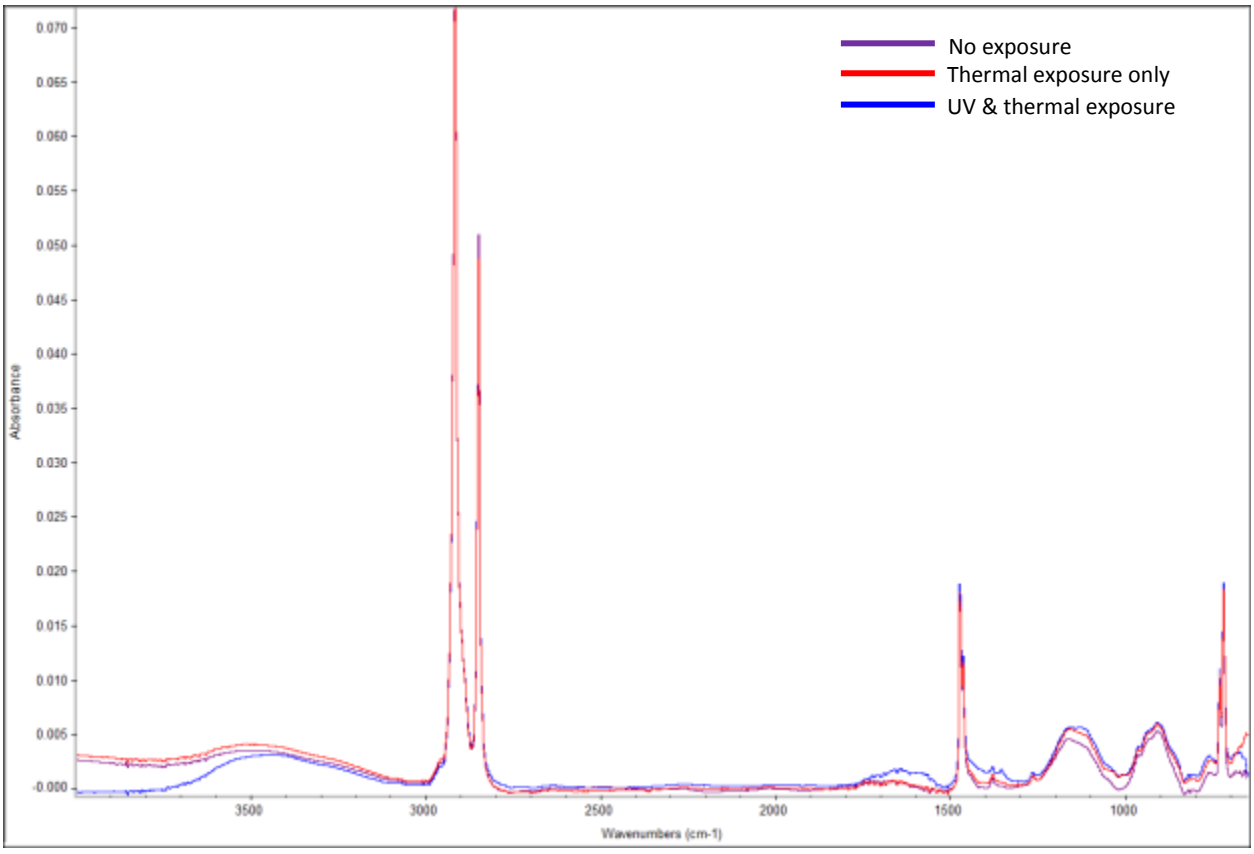

Figure 19: ATR-FTIR spectra of HDPE nurdles used in experiment 1: UV & thermal stress

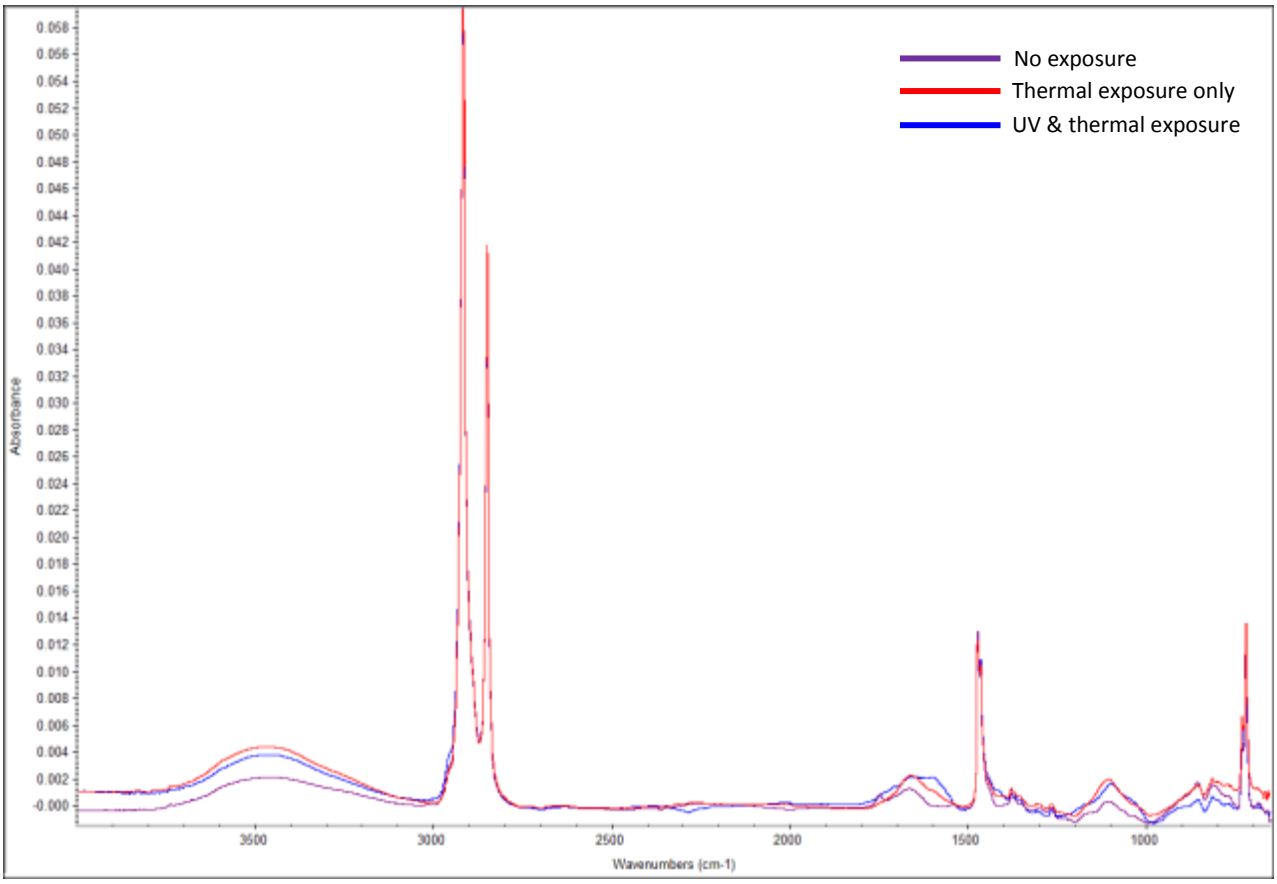

Figure 20: ATR-FTIR spectra of LDPE nurdles used in experiment 1: UV & thermal stress

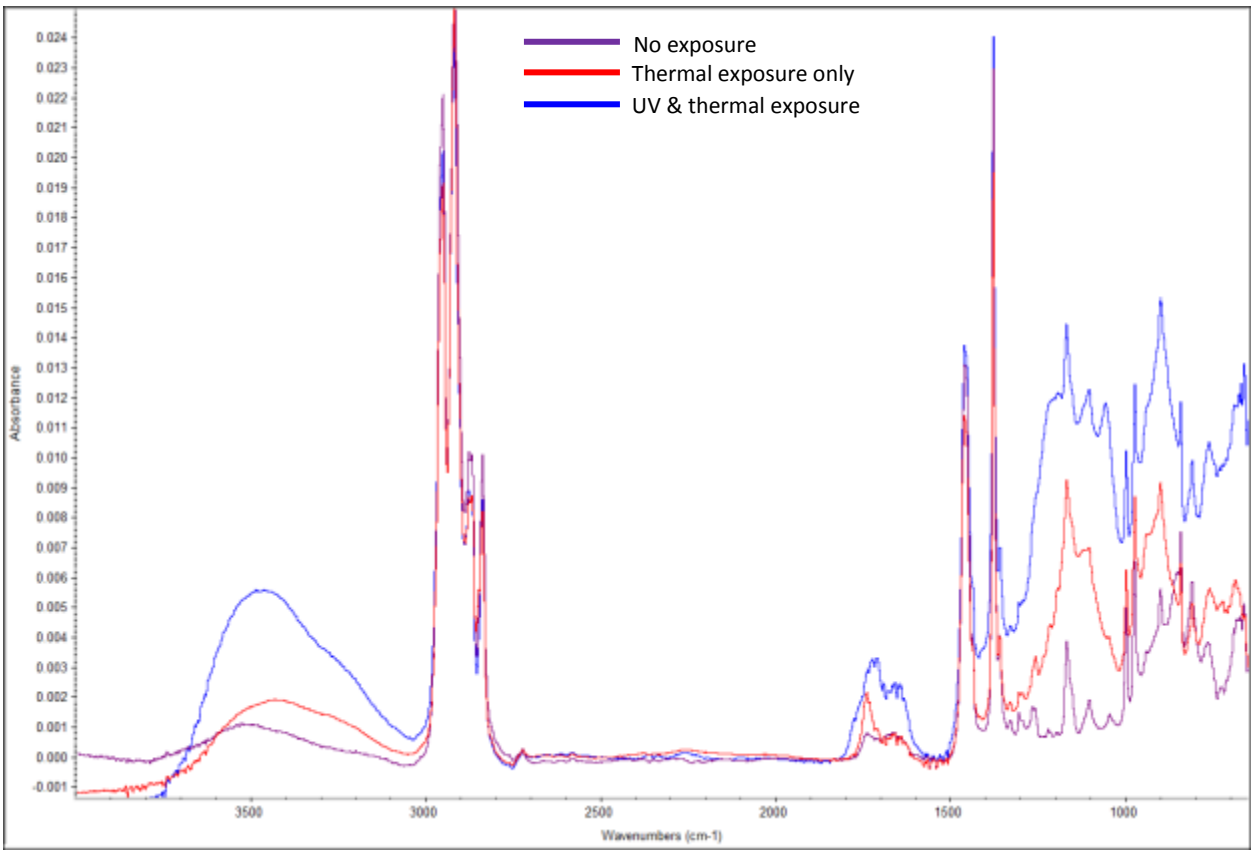

Figure 21: ATR-FTIR spectra of PP nurdles used in experiment 1: UV & thermal stress

Appendix E

Table 12: Raw data for experiment 2: mechanical stress of weight and sieve count

	Weight (g)			Seive Count				
				4 mm		2 mm		
Description	**Pre-treatmen**	**Post-treatmen**	**% Change pre to post**	**Pre-treatmen**	**Post-treatmen**	**Pre-treatmen**	**Post-treatmen**	**% Change in 2mm sieve count**
1 week, no sand	1.3167	1.3256	0.0068	7	7	44	44	0.000
1 week, no sand A	1.3137	1.2785	-0.0268	6	6	45	45	0.000
1 week, sand	1.38	1.3881	0.0059	11	9	43	45	0.047
1 week, sand A	1.38	1.3894	0.0068	9	8	43	44	0.023
1 week, control, no sand	1.37	1.423	0.0387	16	9	38	45	0.184
1 week, control, sand	1.36	1.33	-0.0221	8	5	44	47	0.068
2 week, no sand	1.37	1.3394	-0.0223	19	11	31	39	0.258
2 week, no sand A	1.33	1.2752	-0.0412	19	5	30	44	0.467
2 week, sand	1.3185	1.3394	0.0159	5	3	45	47	0.044
2 week, sand A	1.3199	1.3408	0.0158	9	6	49	43	-0.122
2 week, control, no sand	1.34	1.3467	0.0050	6	4	49	51	0.041
2 week, control, sand	1.3214	1.3256	0.0032	6	6	47	47	0.000
4 week, no sand	1.36	1.3555	-0.0033	18	8	34	44	0.294
4 week, no sand A	1.34	1.4122	0.0539	16	10	36	42	0.167
4 week, sand	1.3255	1.349	0.0177	7	6	43	44	0.023
4 week, sand A	1.3286	1.3653	0.0276	9	9	42	42	0.000
4 week, control, no sand	1.3065	1.3113	0.0037	9	7	39	41	0.051
4 week, control, sand	1.3066	1.3158	0.0070	5	6	51	50	-0.020
8 week, no sand	1.3113	1.3163	0.0038	6	4	46	48	0.043
8 week, no sand A	1.3208	1.3258	0.0038	8	6	41	43	0.049
8 week, sand	1.3218	1.3585	0.0278	3	2	49	50	0.020
8 week, sand A	1.3092	1.3386	0.0225	6	4	48	50	0.042
8 week, control, no sand	1.3068	1.3138	0.0054	5	4	47	48	0.021
8 week, control, sand	1.3094	1.2983	-0.0085	5	6	47	46	-0.021
Average:	1.3319	1.3401	0.0061	9.1	6.3	43.0	45.4	0.070
Standard deviation:	0.0246	0.0369	0.0210	4.8	2.3	5.7	3.1	0.124
95% confidence interval:	0.0098	0.0148	0.0084	1.9	0.9	2.3	1.2	0.049

Table 13: Raw data for experiment 2: mechanical stress of fiber count

	2 micron Filter				0.45 micron Filter			
	Colored Fiber Count		Clear Fiber Count		Colored Fiber Count		Clear Fiber Count	
Description	Pre-treatment	Post-treatment	Pre-treatment	Post-treatment	Pre-treatment	Post-treatment	Pre-treatment	Post-treatment
1 week, no sand	7	9	8	15	6	11	29	34
1 week, no sand A	11	6	12	6	4	4	20	31
1 week, sand	4	15	6	7	5	14	4	2
1 week, sand A	10	7	9	5	3	2	5	0
1 week, control, no sand	9	10	2	15	6	7	30	5
1 week, control, sand	10	5	15	12	7	2	5	5
2 week, no sand	1	5	14	21	2	2	35	31
2 week, no sand A	0	1	14	13	3	3	30	30
2 week, sand	5	14	9	11	8	4	5	6
2 week, sand A	9	6	7	10	10	17	33	32
2 week, control, no sand	11	12	24	10	4	3	56	6
2 week, control, sand	5	4	10	14	2	7	11	25
4 week, no sand	10	5	34	6	6	10	43	12
4 week, no sand A	8	7	18	3	2	7	43	19
4 week, sand	4	4	8	5	10	8	9	5
4 week, sand A	7	5	10	14	11	8	13	5
4 week, control, no sand	9	7	2	11	5	5	17	18
4 week, control, sand	10	5	18	3	6	4	6	12
8 week, no sand	16	3	10	7	6	6	17	14
8 week, no sand A	14	8	10	10	10	5	11	11
8 week, sand	7	11	9	11	4	11	7	24
8 week, sand A	9	11	12	11	8	11	7	24
8 week, control, no sand	8	5	9	7	4	5	12	11
8 week, control, sand	19	6	13	8	19	10	3	9
1 week, no sand control	4	3	6	21	7	7	15	34
1 week, no sand control A	1	4	7	6	8	12	21	37
1 week, sand control	8	10	11	17	6	5	11	12
1 week, sand control A	6	7	14	26	10	1	14	14
nanopur through filters	8		9		4		22	
Average:	7.93	6.96	11.38	10.89	6.41	6.82	18.41	16.71
Standard deviation:	4.28	3.42	6.44	5.61	3.60	3.98	13.95	11.37
95% confidence interval:	1.56	1.27	2.35	2.08	1.31	1.47	5.08	4.21

Table 14: Raw data for experiment 2: mechanical stress for DLS

	100-1000nm diameter range				0 - 100nm diameter range				1000-5500nm diameter range			
	Pre-treatment		Post-treatment		Pre-treatment		Post-treatment		Pre-treatment		Post-treatment	
Description	**Average Peak (nm)**	**% Intensity**	**Average Peak (nm)**	**% Intensity**	**Average Peak (nm)**	**% Intensity**	**Average Peak (nm)**	**% Intensity**	**Average Peak (nm)**	**% Intensity**	**Average Peak (nm)**	**% Intensity**
1 week, no sand	266.66	53.13%	960.8	100%	1.3518	15.27%			5393.45	17.35%		
1 week, no sand A	273.94	100%	168.11	93.63%			0.212	5.50%			1824.83	0.87%
1 week, sand	239.42	100%	428.68	100%								
1 week, sand A	321.71	99.70%	232.97	100%					1671.21	0.30%		
1 week, control, no sand	229.37	90.08%	383.85	93.07%	0.2997	9.23%	0.2279	6.93%	1216.02	0.68%		
1 week, control, sand	260.63	100%	324.42	91.57%			0.5103	6.33%				
2 week, no sand	128.47	41.73%	314.77	100%	0.6483	55.45%			844.33	1.53%		
2 week, no sand A	301.84	39.33%	514.87	45.17%	0.7096	44.20%	0.6592	20.53%	5280.16	16.43%	1325.41	34.30%
2 week, sand	470.09	94.53%	378.45	100%	0.1993	5.47%						
2 week, sand A	922.47	100%	275.42	100%								
2 week, control, no sand	182.39	97.16%	500.82	97.33%	0.1768	2.83%	0.1815	2.66%				
2 week, control, sand	142.64	100%	98.322	100%								
4 week, no sand	273.12	100%	170.18	74.13%			0.4879	25.87%				
4 week, no sand A	205.19	100%	781.02	92.03%			0.1873	3.70%			1416	4.27%
4 week, sand		0%	471.24	100%					1671.29	100%		
4 week, sand A	327.31	100%	527.62	100%								
4 week, control, no sand	254.6	97.40%	252.57	82.47%	0.2331	2.60%	0.4369	12.41%			817.52	3.59%
4 week, control, sand	254.6	97.40%	137.03	100%	0.2331	2.60%						
8 week, no sand	501.47	98.49%	190.15	57.10%	0.1641	1.51%	43.06	40.57%			0.1892	2.33%
8 week, no sand A	441.79	100%	567.29	100%								
8 week, sand	389.29	88.89%	468.27	100%	0.8054	11.11%						
8 week, sand A	522.05	79.73%	931.1	100%	0.3076	6.48%			1555.43	13.78%		
8 week, control, no sand	370.61	100%	967.6	100%								
8 week, control, sand	314.93	100%	297.04	91.37%			0.5775	7.22%				
1 week, no sand control	383.89	100%	177.51	57.60%			0.7875	37.43%			1591.05	4.97%
1 week, no sand control A	217.32	100%	635.95	100%								
1 week, sand control			361.61	100%								
1 week, sand control A			210.09	100%								
nanopur through filters			190.9	100%								
nano5.26			317.82	89.83%							2092.3	10.17%
Average:		87.6%		92.2%								
Standard deviation:		25.3%		14.6%								
95% confidence interval:		9.9%		5.2%								

Appendix F

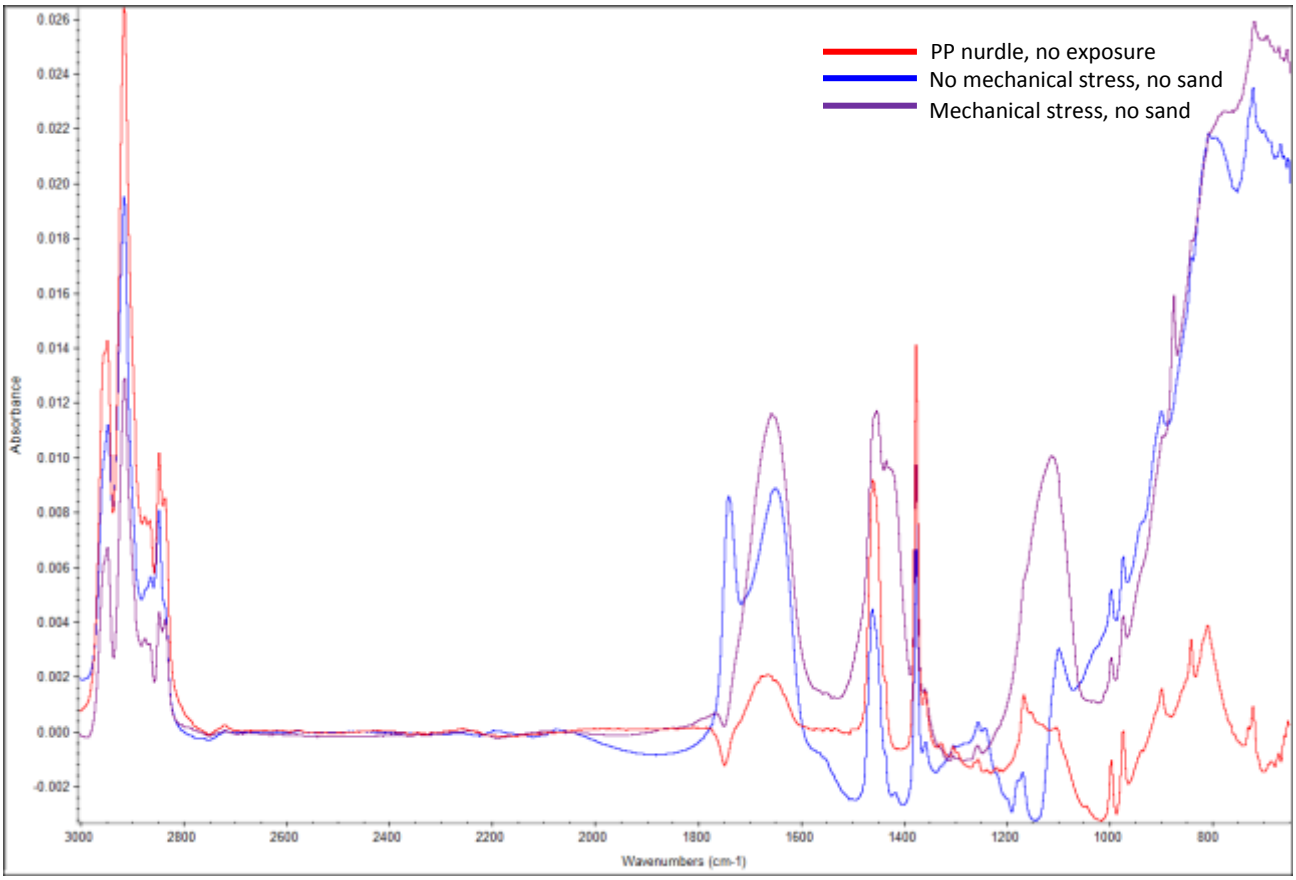

Figure 22: ATR-FTIR spectra of PP nurdles used in experiment 2: mechanical stress, after 1 week exposure

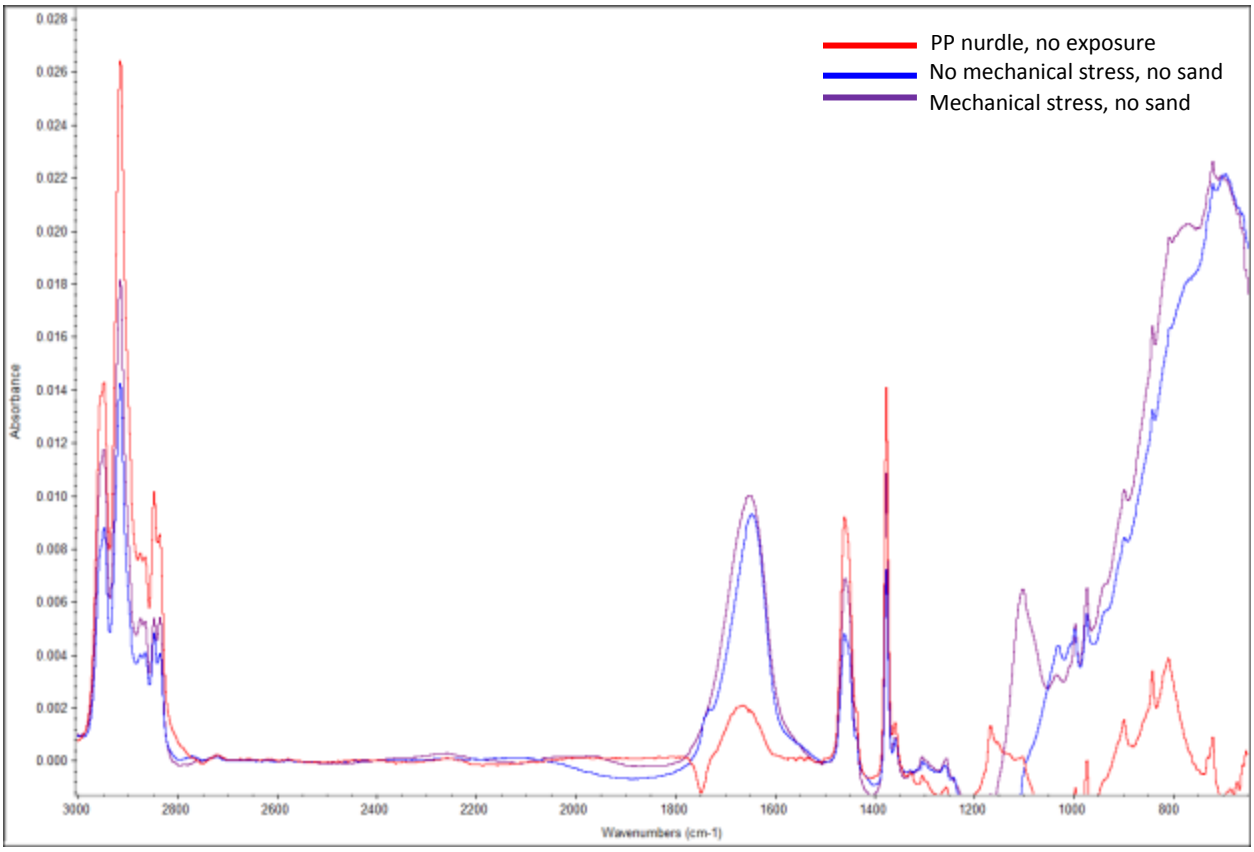

Figure 23: ATR-FTIR spectra of PP nurdles used in experiment 2: mechanical stress, after 8 weeks exposure